EPS-HEP2023, 23 AUGUST 2023

Vector boson scattering measurements in ATLAS and CMS

Matteo Presilla
(Karlsruhe Institute of Technology)
on behalf of the ATLAS and CMS Collaborations

Standard model precision measurements

LHC as a **precision** machine: diagrams in which two Vector Boson interacts, giving either one or two Vector Bosons in the final state, are among the rarest processed measured

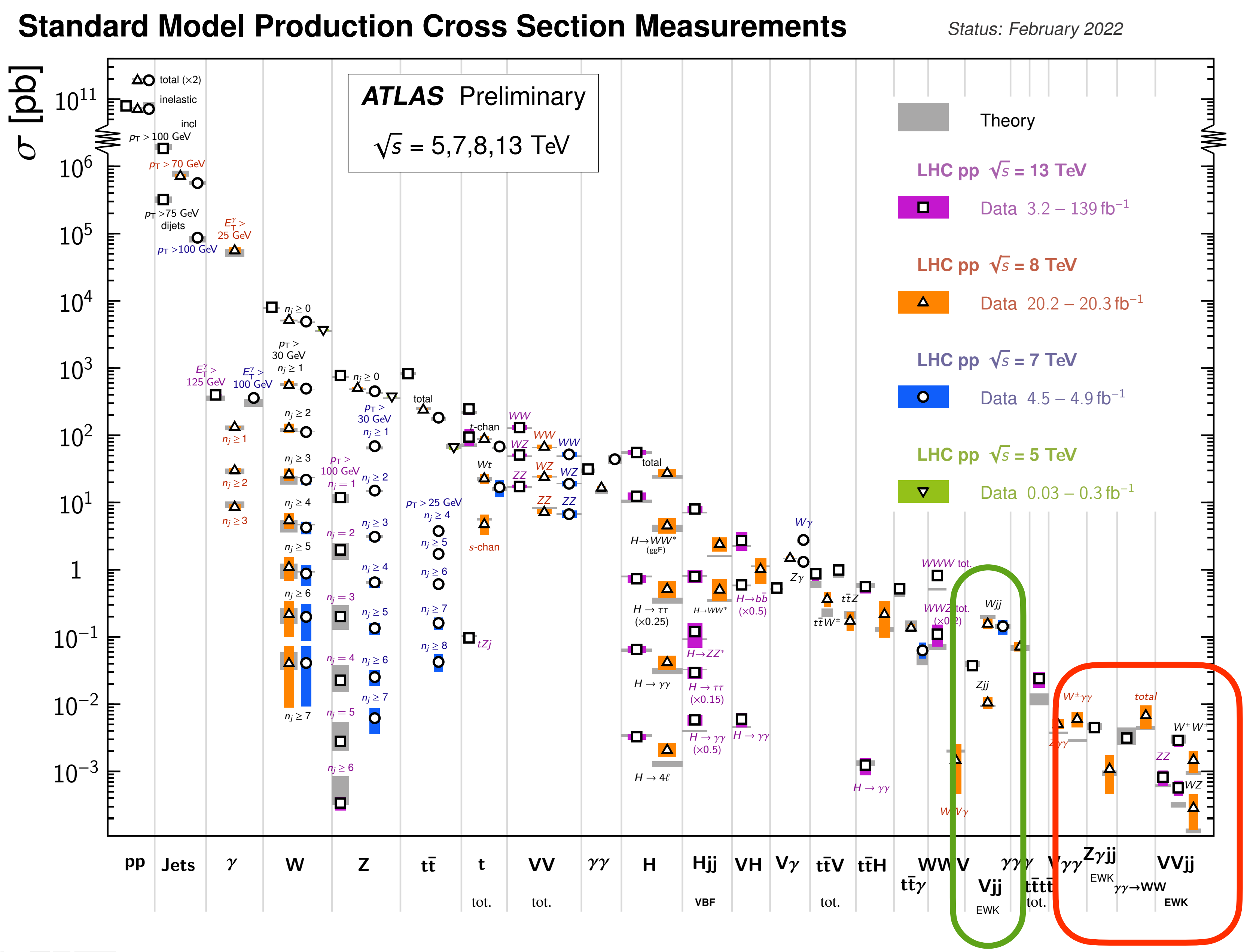

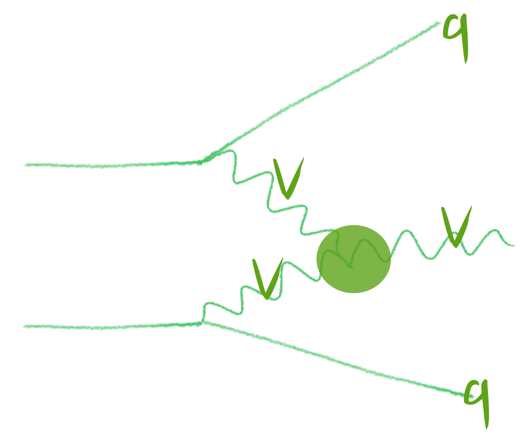

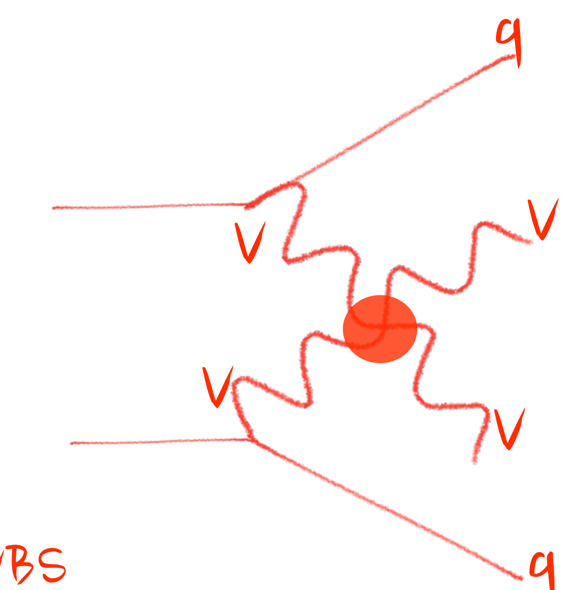

VBF & VBS
EW processes

ATL-PHYS-PUB-2022-009

Physics of VBS processes

- **At the heart of EWSB, probing non-abelian EW structure of the SM:** triple and quartic gauge couplings

Physics of VBS processes

- **At the heart of EWSB, probing non-abelian EW structure of the SM:** triple and quartic gauge couplings

- **Studies of gauge invariance of the SM**: this process is gauge invariant thanks to very delicate cancellations between diagrams

Physics of VBS processes

- **At the heart of EWSB, probing non-abelian EW structure of the SM:** triple and quartic gauge couplings
- **Studies of gauge invariance of the SM**: this process is gauge invariant thanks to very delicate cancellations between diagrams
- **Unitarity of the SM:** VBS amplitude *explodes* with energy, without H mediation!

Undergrad typical QFT exercise:

SCATTERING $Z_L Z_L \Longleftrightarrow W^+_L W^-_L$

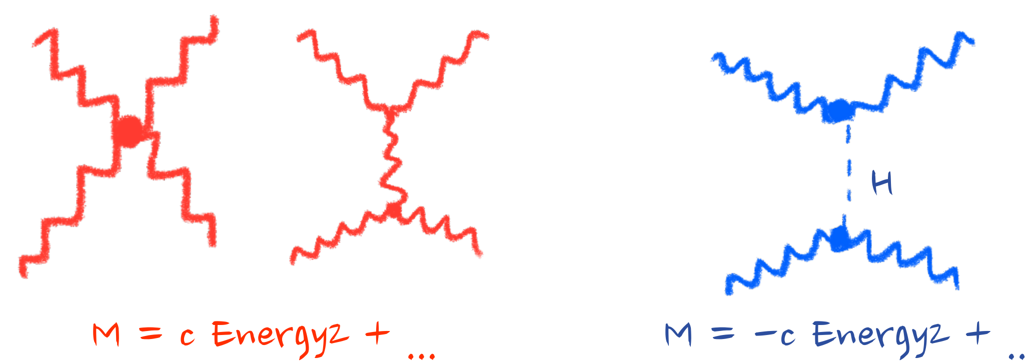

Higgs exchange cancels high-energy growth if its couplings are SM-like, matrix element is unitary for $m_H \lesssim 1\text{TeV}$

(*Lee, Quigg, Thacker bound*)

Physics of VBS processes

- **Powerful portal to access BSM** in a model-independent approach, usually parametrizing deviations from SM as Effective Field Theory (EFT) expansion

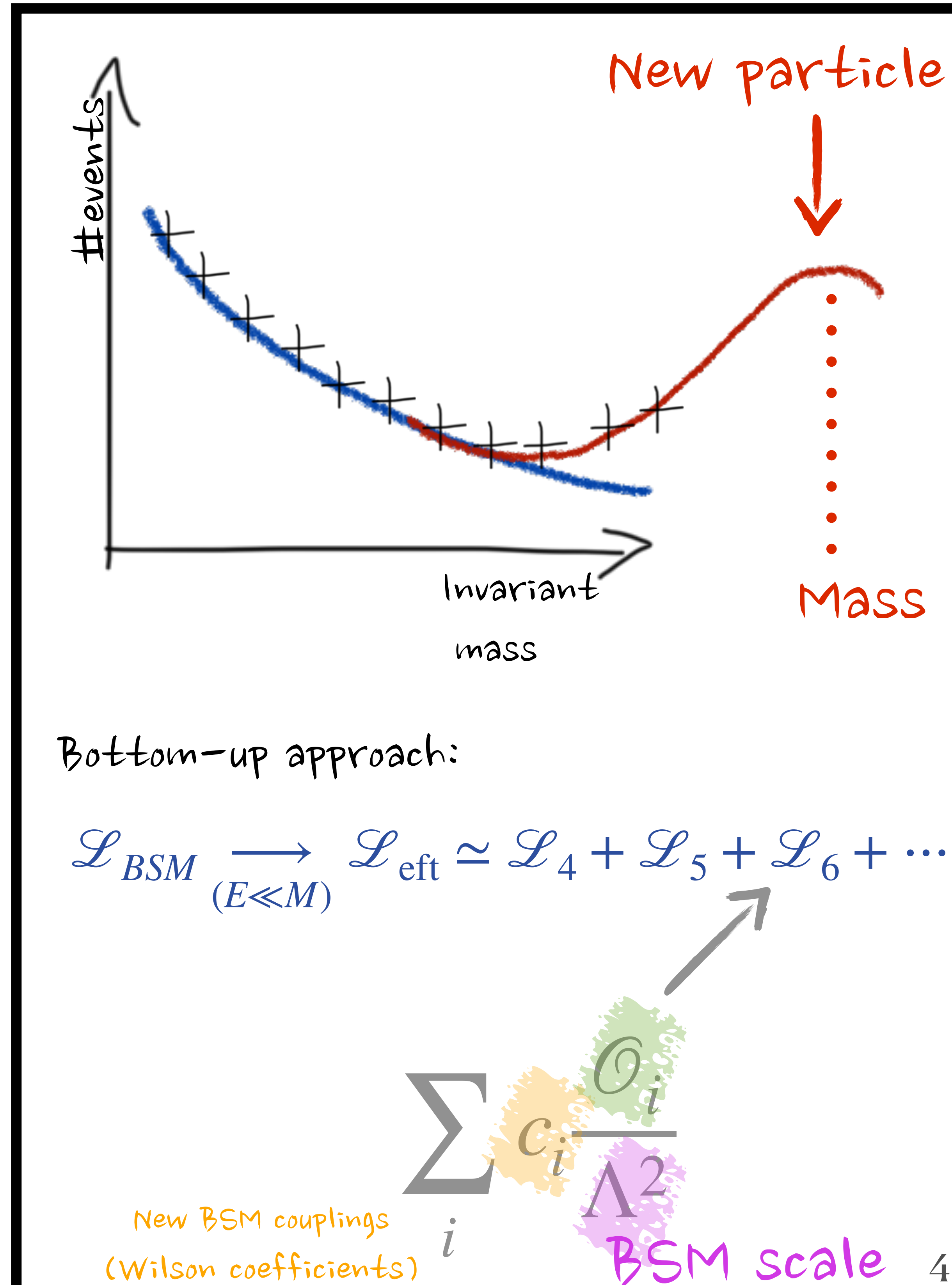

Physics of VBS processes

- **Powerful portal to access BSM** in a model-independent approach, usually parametrizing deviations from SM as Effective Field Theory (EFT) expansion

$$\mathcal{O}_{S,0} = \left[(D_\mu\Phi)^\dagger D_\nu\Phi\right] \times \left[(D^\mu\Phi)^\dagger D^\nu\Phi\right]$$
$$\mathcal{O}_{S,1} = \left[(D_\mu\Phi)^\dagger D^\mu\Phi\right] \times \left[(D_\nu\Phi)^\dagger D^\nu\Phi\right]$$
$$\mathcal{O}_{S,2} = \left[(D_\mu\Phi)^\dagger D_\nu\Phi\right] \times \left[(D^\nu\Phi)^\dagger D^\mu\Phi\right]$$

$$\mathcal{O}_{M,0} = \mathrm{Tr}\left[\widehat{W}_{\mu\nu}\widehat{W}^{\mu\nu}\right] \times \left[(D_\beta\Phi)^\dagger D^\beta\Phi\right]$$
$$\mathcal{O}_{M,1} = \mathrm{Tr}\left[\widehat{W}_{\mu\nu}\widehat{W}^{\nu\beta}\right] \times \left[(D_\beta\Phi)^\dagger D^\mu\Phi\right]$$
$$\mathcal{O}_{M,2} = \left[\widehat{B}_{\mu\nu}\widehat{B}^{\mu\nu}\right] \times \left[(D_\beta\Phi)^\dagger D^\beta\Phi\right]$$
$$\mathcal{O}_{M,3} = \left[\widehat{B}_{\mu\nu}\widehat{B}^{\nu\beta}\right] \times \left[(D_\beta\Phi)^\dagger D^\mu\Phi\right]$$
$$\mathcal{O}_{M,4} = \left[(D_\mu\Phi)^\dagger \widehat{W}_{\beta\nu} D^\mu\Phi\right] \times \widehat{B}^{\beta\nu}$$
$$\mathcal{O}_{M,5} = \left[(D_\mu\Phi)^\dagger \widehat{W}_{\beta\nu} D^\nu\Phi\right] \times \widehat{B}^{\beta\mu}$$
$$\mathcal{O}_{M,7} = \left[(D_\mu\Phi)^\dagger \widehat{W}_{\beta\nu} \widehat{W}^{\beta\mu} D^\nu\Phi\right]$$
$$\ldots$$

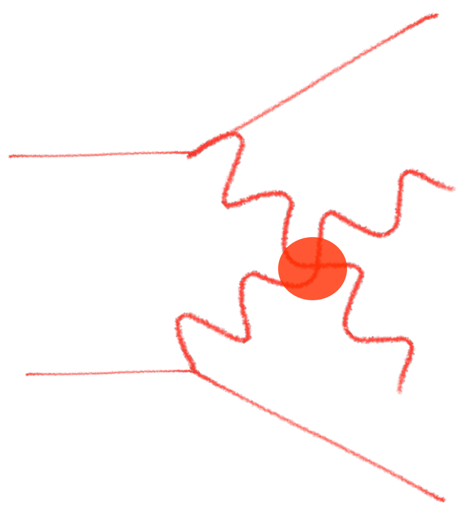

Historically: anomalous quartic gauge couplings (dim-8 EFT)*

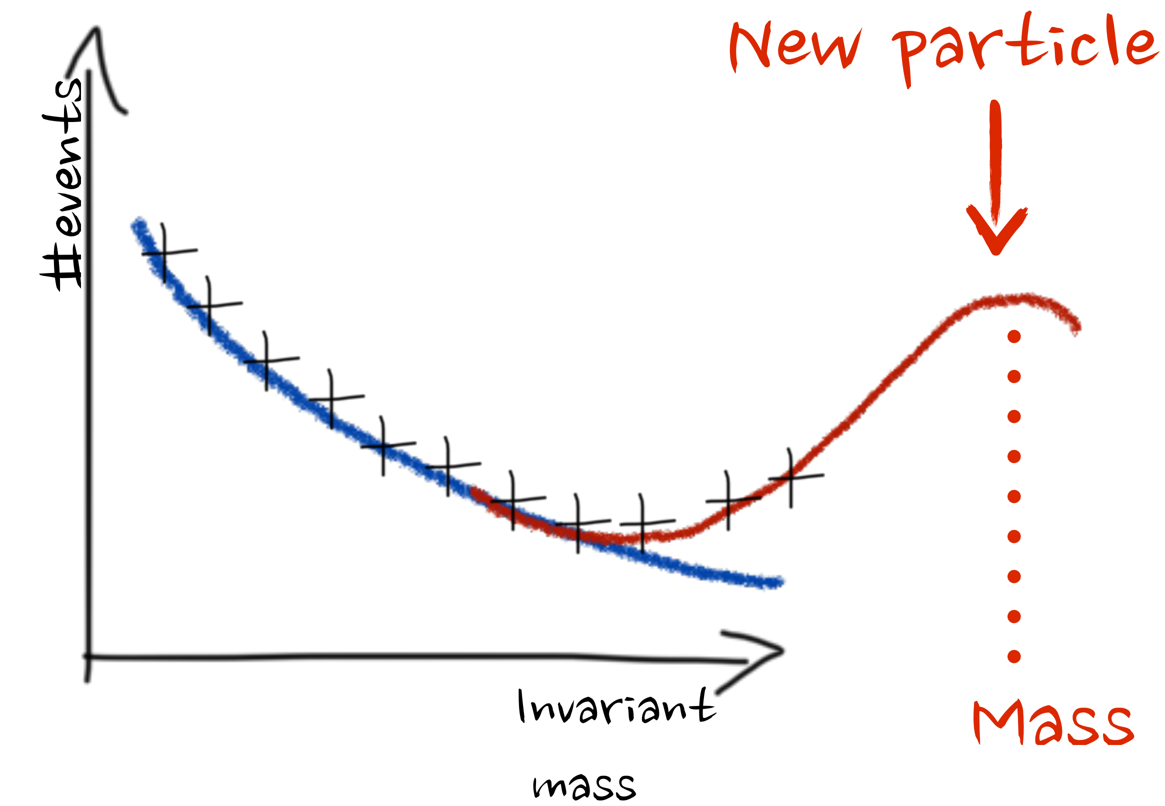

Bottom-up approach:

$$\mathscr{L}_{BSM} \xrightarrow[(E \ll M)]{} \mathscr{L}_{\mathrm{eft}} \simeq \mathscr{L}_4 + \mathscr{L}_5 + \mathscr{L}_6 + \cdots$$

$$\sum_i \frac{c_i \mathcal{O}_i}{\Lambda^2}$$

New BSM couplings (Wilson coefficients)

BSM scale

*Eboli et Al. model

How VBS looks like

THEORY PERSPECTIVE (LO)

- $\mathcal{O}(\alpha_{ew}^6)$ **process: quartic diagrams**
  + gauge invariant diagrams
- $\mathcal{O}(\alpha_s^2\alpha_{ew}^4)$ QCD induced process

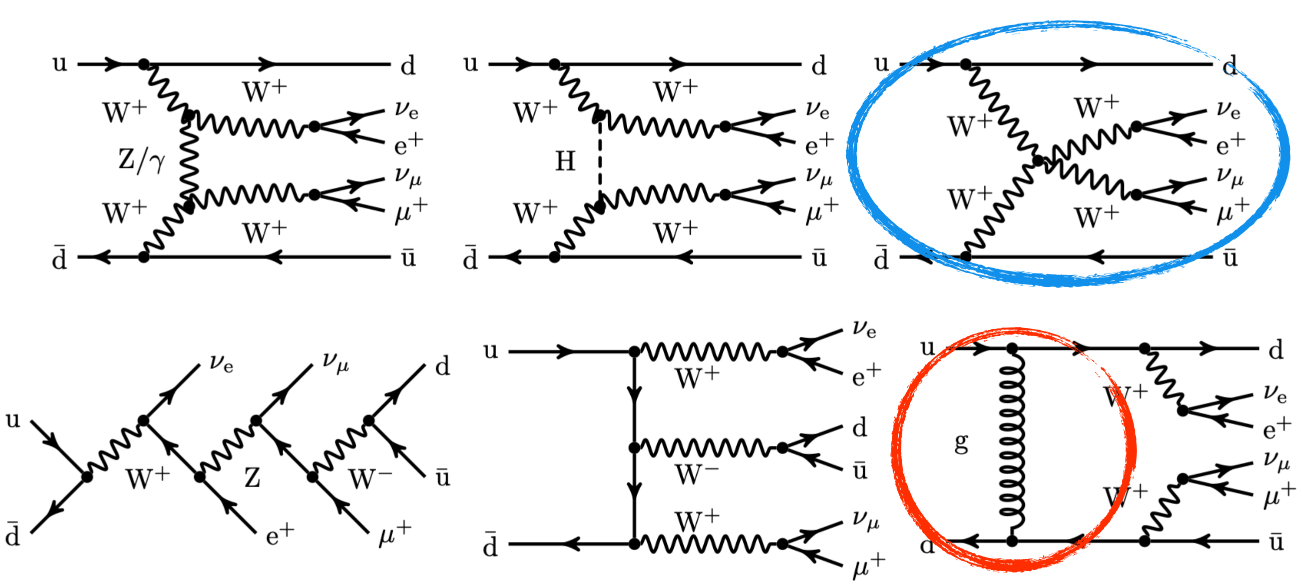

https://arxiv.org/pdf/1708.00268.pdf

How VBS looks like

THEORY PERSPECTIVE (LO)

- $\mathcal{O}(\alpha_{ew}^6)$ **process: quartic diagrams**
  + gauge invariant diagrams
- $\mathcal{O}(\alpha_s^2\alpha_{ew}^4)$ QCD induced process

https://arxiv.org/pdf/1708.00268.pdf

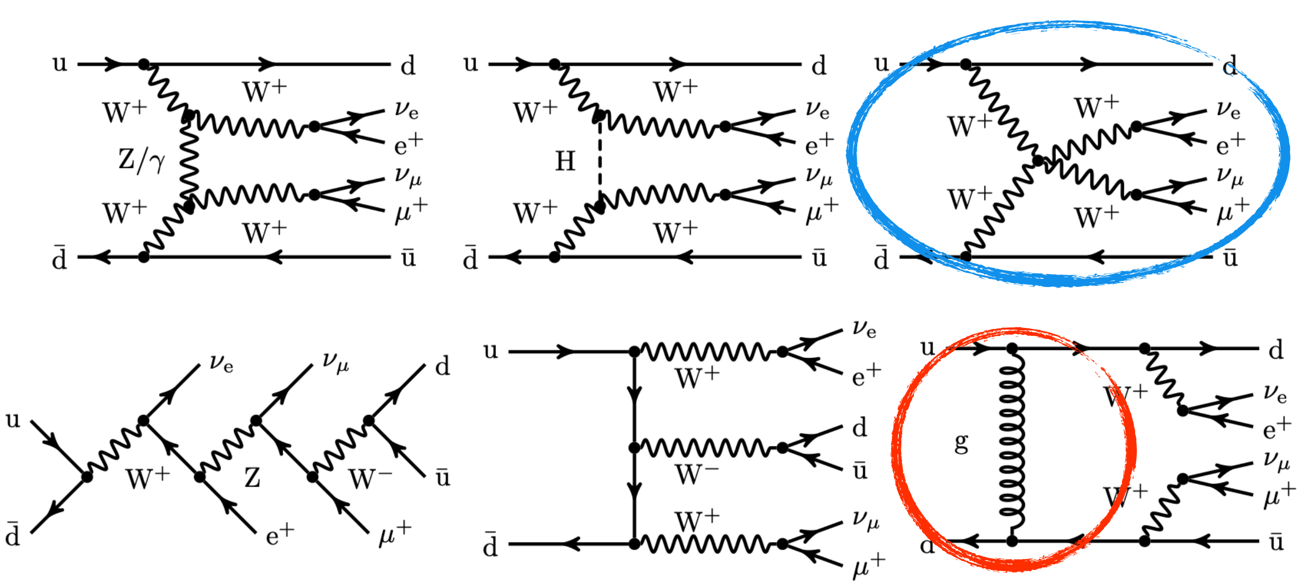

EXP. PERSPECTIVE

- Vector Bosons produced in the central part of the detector
- VBS "**tag-jets**" in **forward** detector region: **highest invariant-mass** in the event
- **Large pseudorapidity separation** between the VBS-jets - for the low QCD activity btw partons
  (no color flow at LO arXiv. 1805.09335)

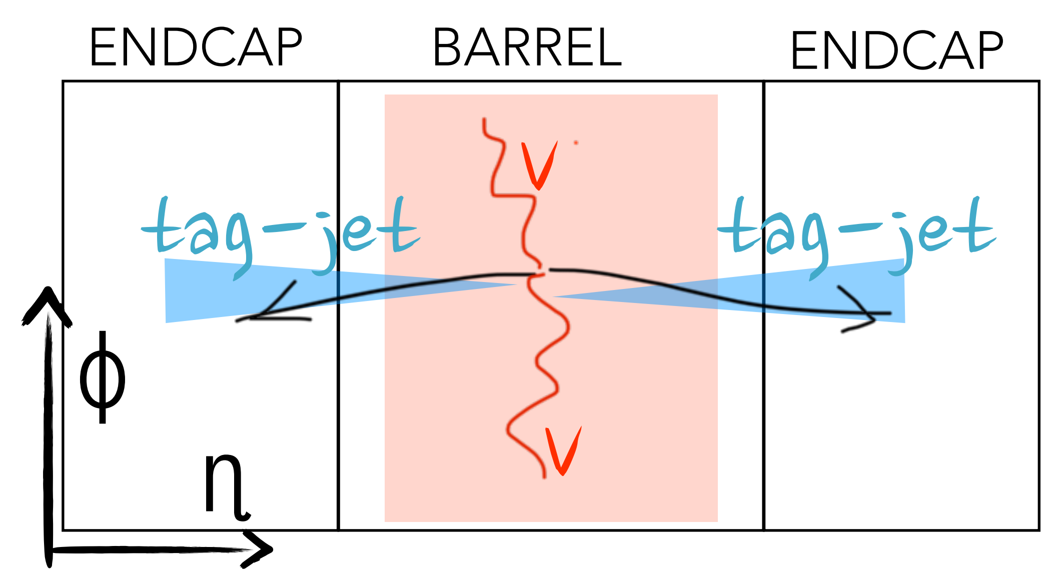

VBS EVENT TOPOLOGY

Recent results

CMS

PROCESS	RESULTS	REFERENCE
polarized ssWW	$W_L W_L$ measurement	PLB 812 (2020) 136018
ZZ (4ljj)	4.0 σ + dim-8 EFT limits	PLB 812 (2021) 135992
osWW (2l2νjj)	Observation + XS	PLB 841 (2023) 137495
★★ **ssWW to τ_h**	**2.7 σ**	**CMS-PAS-SMP-22-008**
Wγ	Observation, differential XS + dim-8 EFT	PLB 811 (2020) 135988 + arXiv:2212.12592
VBS Zγ	Observation	PRD.104.072001
★ **VV semi-leptonic**	**WVjj evidence with full Run2 data**	**PLB 834 (2022) 137438**
VVpp (4jpp)	Dim-6/8 QGCs (100/fb CMS+TOTEM)	JHEP 07 (2023) 229

ATLAS EXPERIMENT

PROCESS	RESULTS	REFERENCE
Zγ (2νγjj)	Observation + dim-8 EFT	JHEP 06 (2023) 082
Zγ (2lγjj)	Observation + XS + differential XS	arXiv:2305.19142 ★
ZZ (4ljj)	Diff. XS+ dim-8 EFT	ATLAS-CONF-2023-024 ★
osWW (2l2νjj)	**Observation + XS**	**ATLAS-CONF-2023-039** ★
ssWW + WZ	Combined EFT interpretation (36/fb)	ATL-PHYS-PUB-2023-002
ssWW	**Diff. XS + BSM +EFT interpretation**	**ATLAS-CONF-2023-023** ★
ZZ (4ljj, 2νjj)	Observation	Nature Phys. 19 (2023) 237

★ **Focus of this talk**

★ **Newest**

Fully leptonic ssWW

- WW to same-sign lepton pair + jet events, **“golden channel” for VBS** for good separation **EW VBS** vs. **QCD VBS**
  - First observation with 2016 data, recently CMS accessed definite polarization WW scattering [PLB 812 (2021) 136018]
- ATLAS novel measurement profits of an **improved signal modeling**, WZ **background modeling**, and updates in the non-prompt lepton background estimation **+ direct and indirect BSM interpretation**

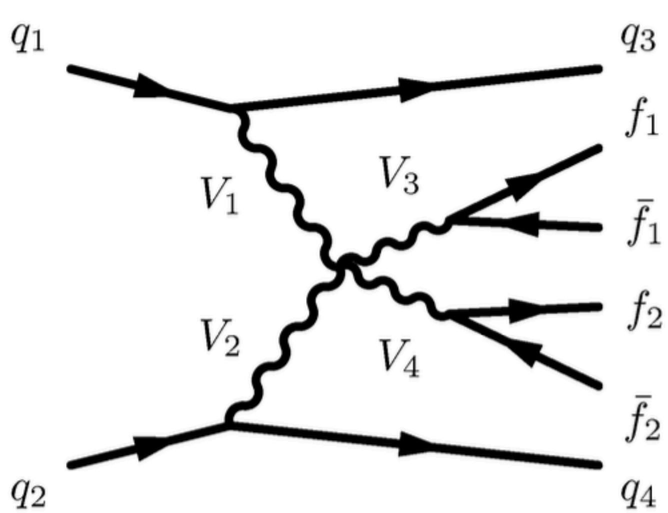

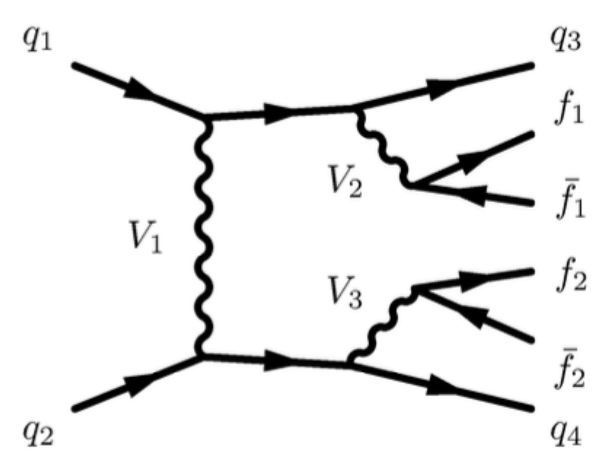

$\sigma_{\mathrm{EW}} \sim$ 4-6 σ_{QCD}

Fully leptonic ssWW

- WW to same-sign lepton pair + jet events, **"golden channel" for VBS** for good separation EW VBS vs. QCD VBS
  - First observation with 2016 data, recently CMS accessed definite polarization WW scattering [PLB 812 (2021) 136018]
- ATLAS novel measurement profits of an **improved signal modeling**, WZ **background modeling**, and updates in the non-prompt lepton background estimation **+ direct and indirect BSM interpretation**

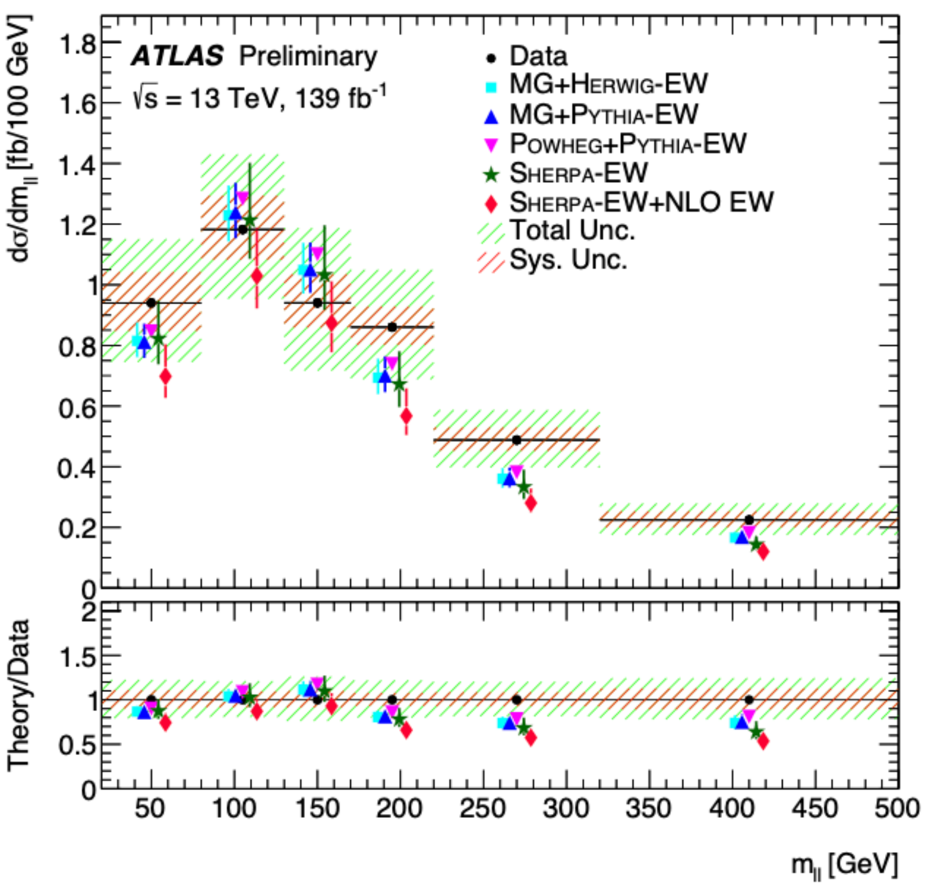

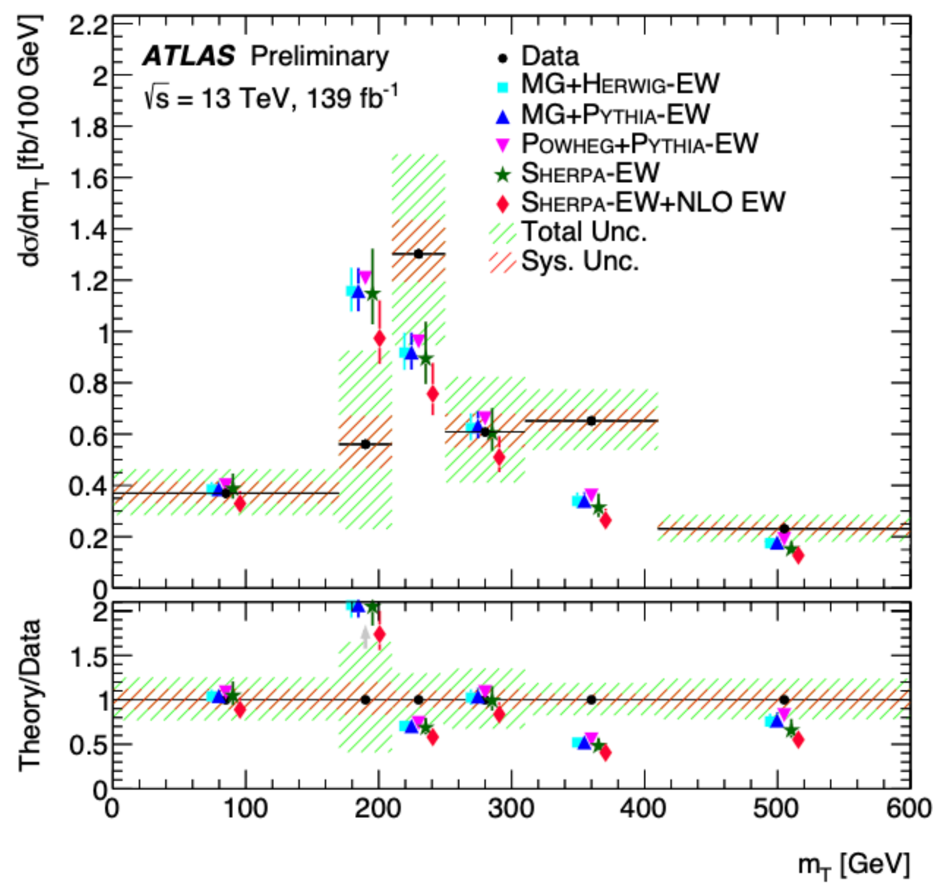

Differential cross sections are compared with the SM predictions from: **MG+Herwig, MG+Pythia**, **Sherpa-EW**, and **NLO Powheg Box + Pythia**

- General good agreement for all variable examined, except for transverse mass
- **Predictions tend to underestimate the data, NLO corrections move the prediction to lower values**

ssWW and BSM

- **Dilepton mass** shows high-sensitivity to NP scenarios in the EFT (dim-8) approach
- Competitive bounds with best-world limits, while preserving **EFT validity**

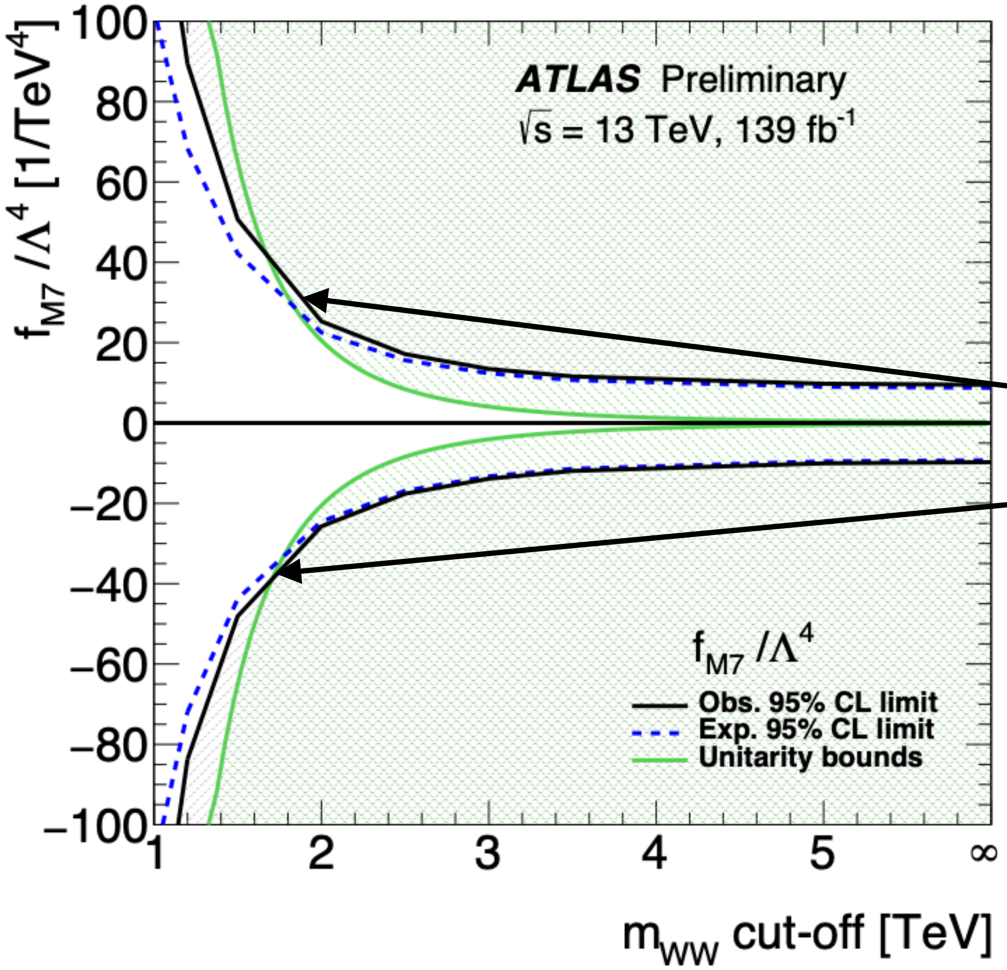

Interplay between **experimental bounds** and **theoretical bounds**

CI for f_{M7} as a **function of a cut-off scale** & **unitarity bounds**

ssWW and BSM

- **Dilepton mass** shows high-sensitivity to NP scenarios in the EFT (dim-8) approach
- Competitive bounds with best-world limits, while preserving **EFT validity**

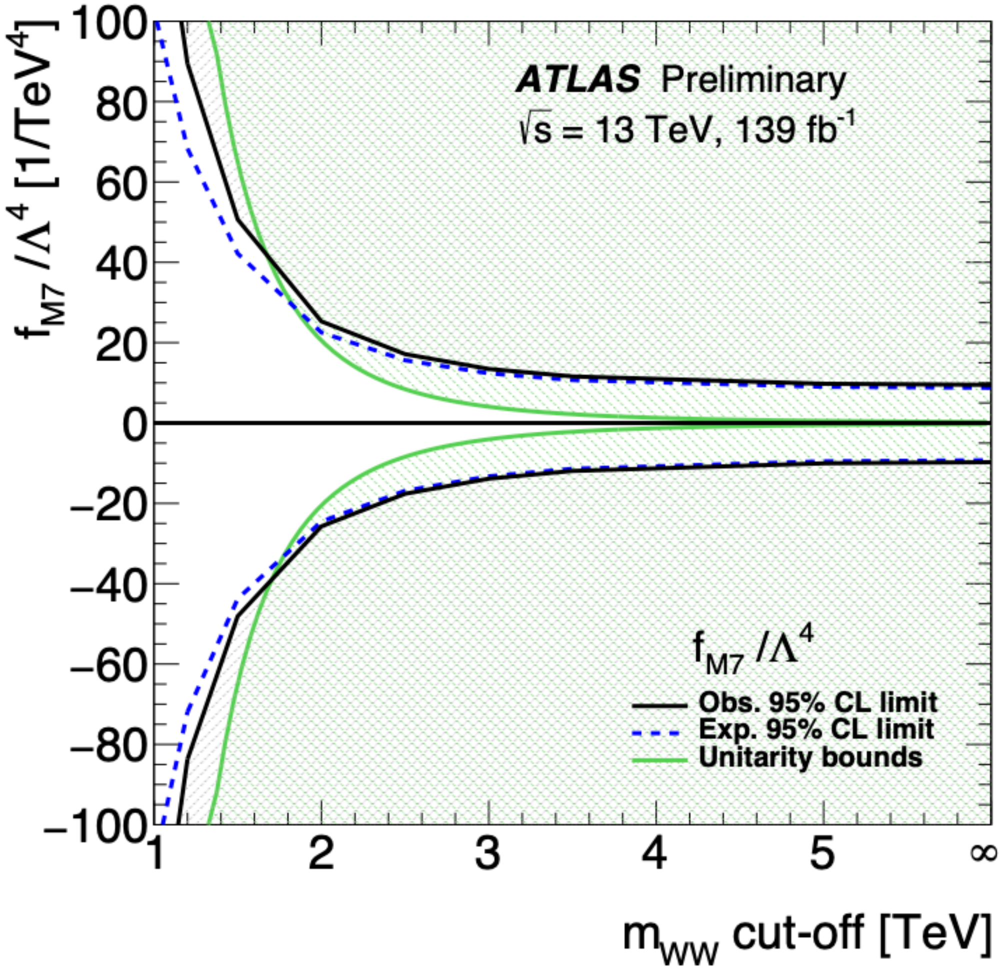

CI for f_{M7} as a **function of a cut-off scale** & **unitarity bounds**

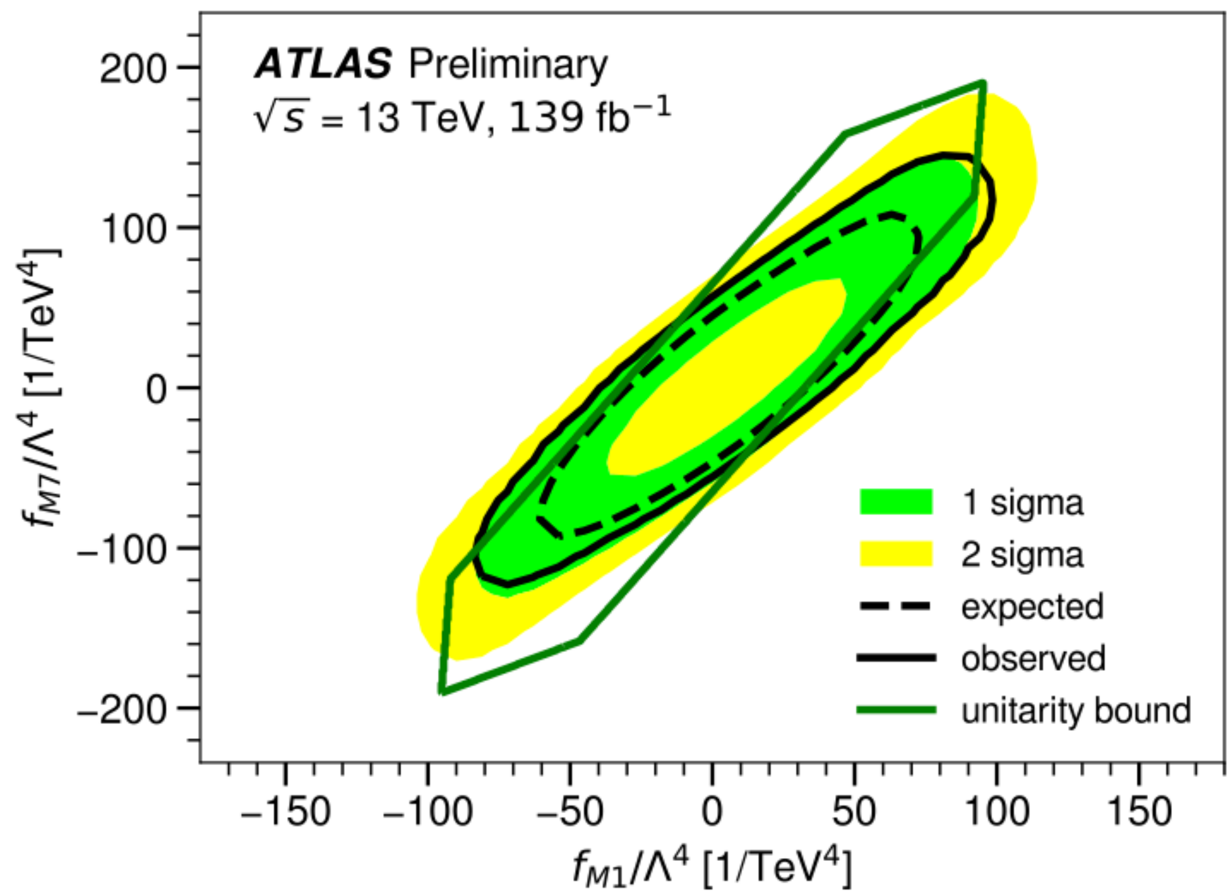

2D limits & perturbative **unitarity bounds**

VBS decaying to tau lepton

$$q\bar{q} \rightarrow W^{\pm}W^{\pm}q\bar{q} \rightarrow \tau_h^{\pm}\nu_\tau\ell^{\pm}\nu_\ell q\bar{q}$$

- Possibility to access **tau decay channel in ssWW VBS** for the **first time**
- Final state: **$\ell^\pm$ $\tau_h^\pm$ jj + MET (ℓ = e, μ)**
- Almost **95% of the background events** in SR contain **nonprompt leptons** from jets misreconstructed as e,μ, or τ_h;
  about **2% are from Z/γ$*$+jets**,
  and **1% from dileptonic** $t\bar{t}$ production

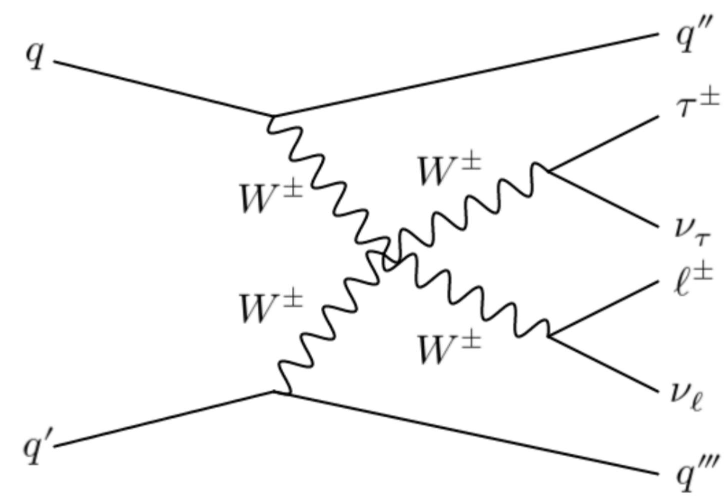

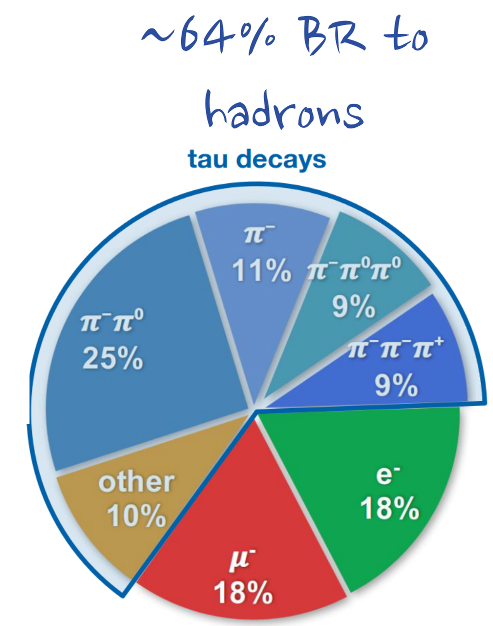

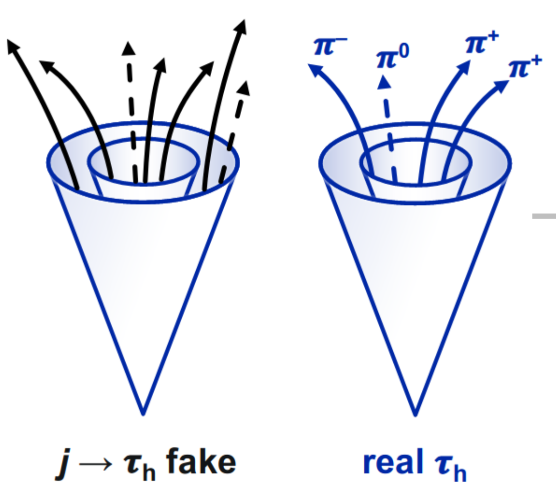

"Nonprompt leptons" background estimated from data, and validated in a CR close to the SR

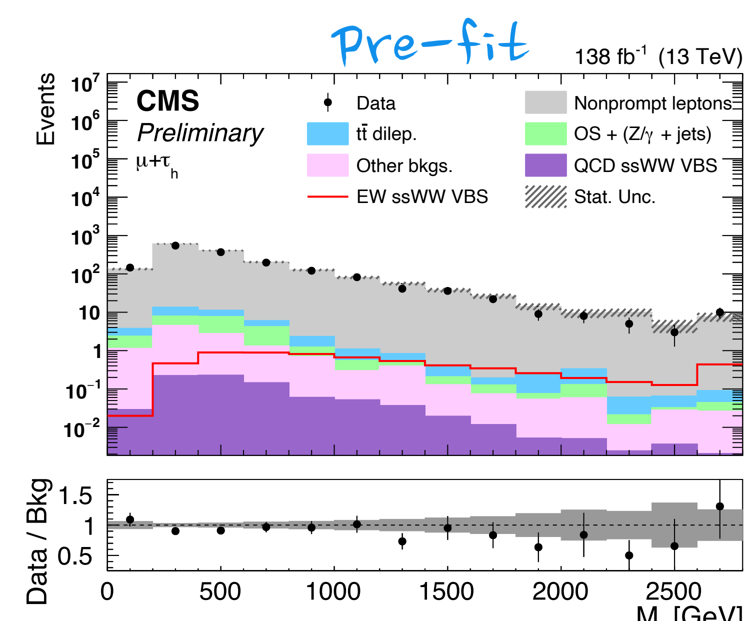

VBS decaying to tau lepton

- 9 kinematic quantities peculiar of the ssWW VBS process as input features of a DNN, trained to classify the events in signal and background categories
- ML fit using DNN templates from **SR** and **two enriched background regions** to control **opposite-sign, ZZ and $t\bar{t}$ rates**
- Two separate measurements:
  - ssWW purely-EW signal strength
  - Simultaneous EW and QCD ssWW signal strength

Signal	Significance [σ] Expected	Significance [σ] Observed
pure EW ssWW VBS	1.9	**2.7**
EW + QCD ssWW VBS	2.0	**2.9**

- The overall **uncertainty is dominated by the statistics** of the data considered

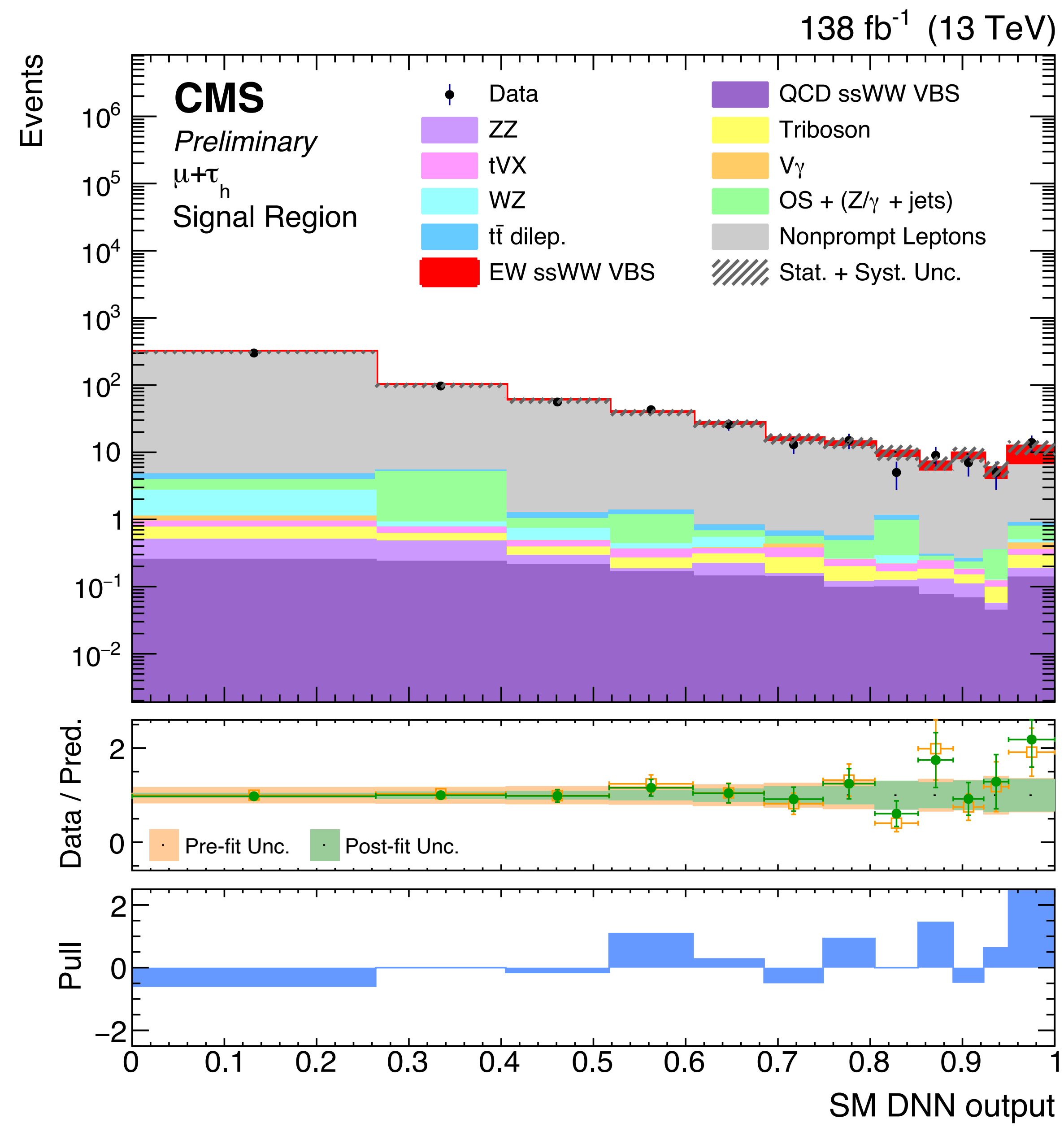

Opposite sign WW

- The W+W− channel is **experimentally challenging** because of the **large $t\bar{t}$ background** that enter the signal selection
- Measured for the first time by CMS [PLB 841 (2023) 137495] with an observed significance of 5.6 σ
- Recently measured by ATLAS using slightly different regions and MC generators

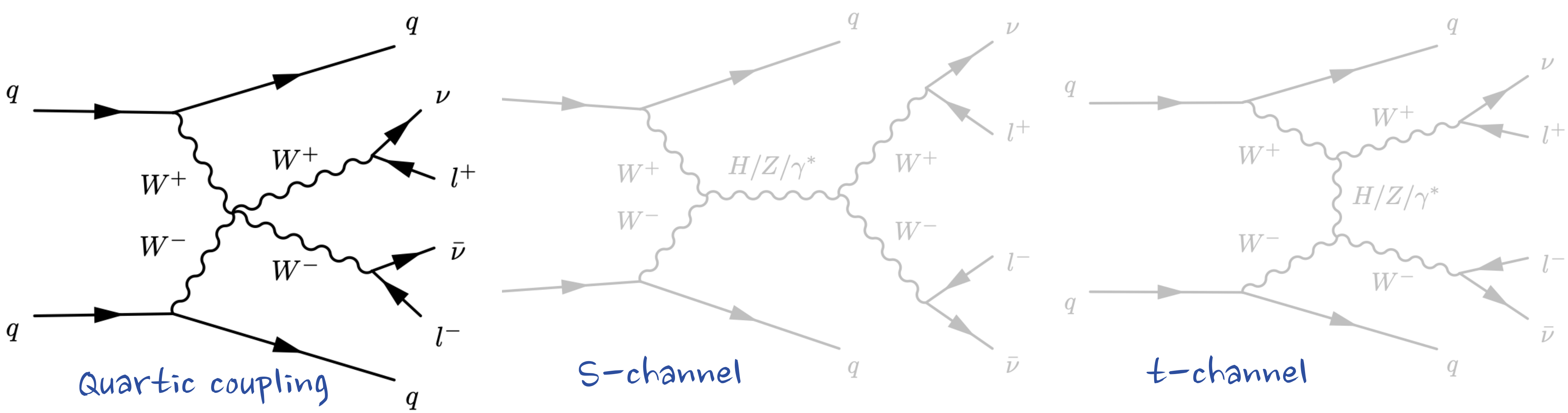

Opposite flavor, positive centrality, 2-3 jets with b-jets veto

Electroweak W+W− jj production at NLO pQCD with **POWHEG-BOX2**

The **Higgs contribution suppressed** by a generator level cut on the EWK invariant mass of the decay leptons and neutrinos. **s-channel contribution are neglected**.

Opposite sign WW

The discrimination between signal and background in the SR is performed by a NN, including both the 2 and 3 jets topologies

- Simultaneous fit in SR and top CR (requiring one of the two leading jets to be a b-jet)
- **floating** normalization btw the regions for **top** and **QCD osWW backgrounds** to measure their normalization

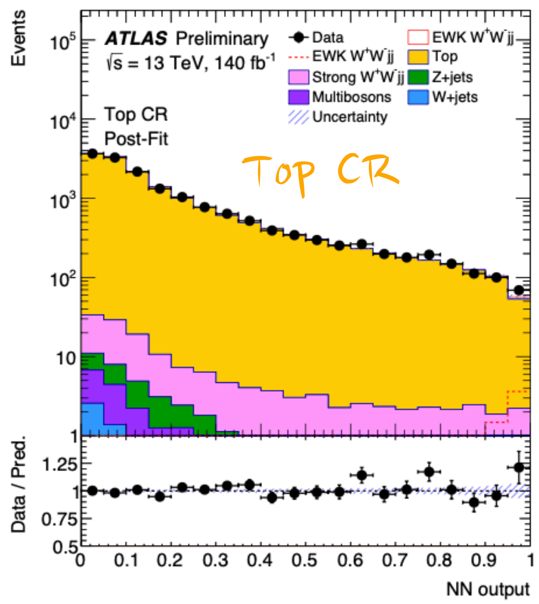

~66% top events

~24% osWW QCD events

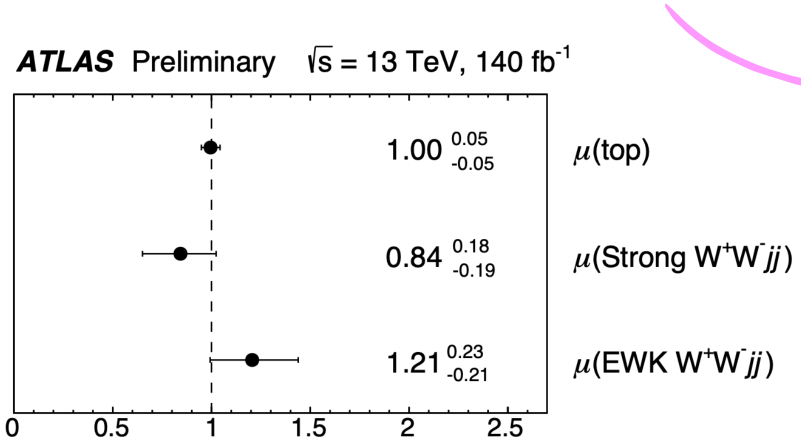

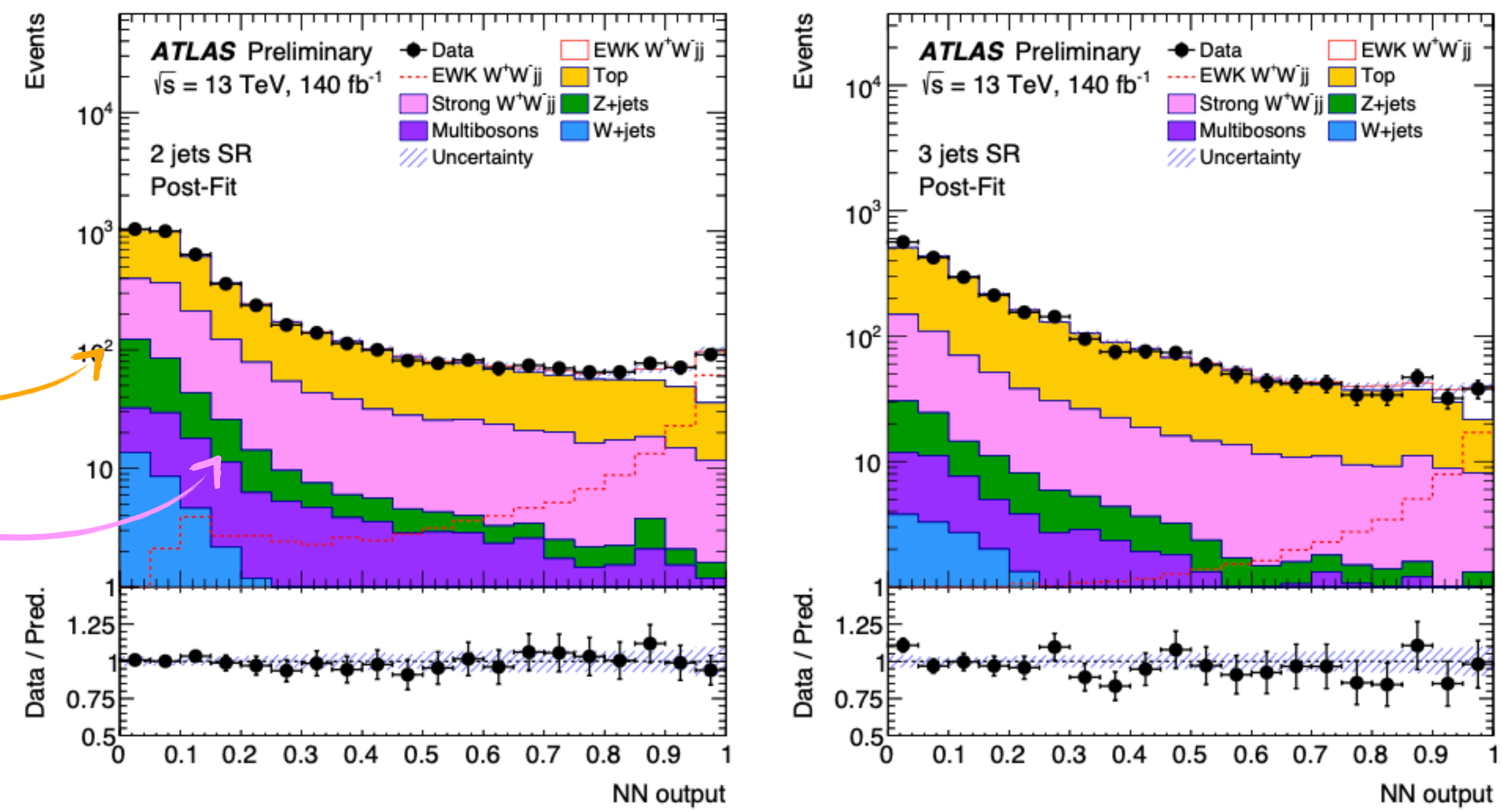

(a) Two jets (b) Three jets

Dominant uncertainty on the fit is due to the **limited statistics in data** and amounts to **12.3%**, while the total uncertainty is 18.5%. The signal has been observed with a **significance of 7.1σ**, (6.2 exp) from the rejection of the background-only hypothesis.

Fiducial cross section measured $2.65^{+0.65}_{-0.48}$ ($2.20^{+0.14}_{-0.13}$ Powheg).

PLB 834 (2022) 137438

Evidence for semi-leptonic VBS decays

Good balance between:

✓ Benefit from the large hadronic branching fraction of W or Z boson

✳ Larger irreducible backgrounds

SIGNAL

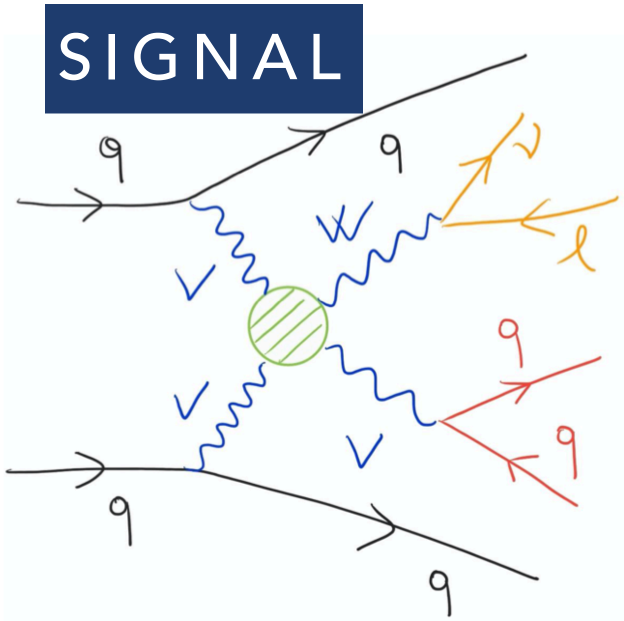

$\mathcal{O}(\alpha_{EW}^6)$

IRREDUCIBLE BACKGROUNDS

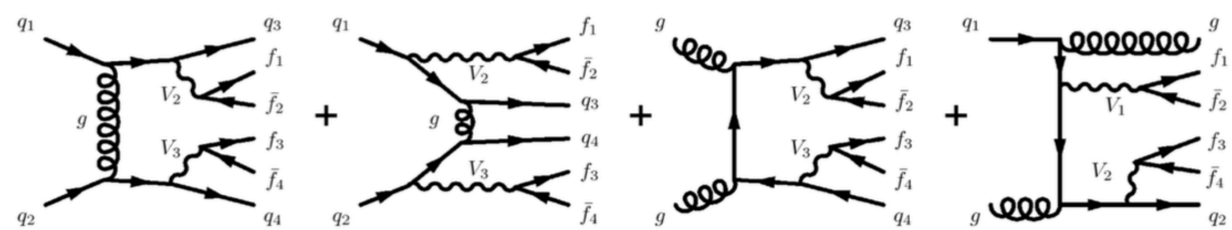

$\mathcal{O}(\alpha_{EW}^4\alpha_S^2)$

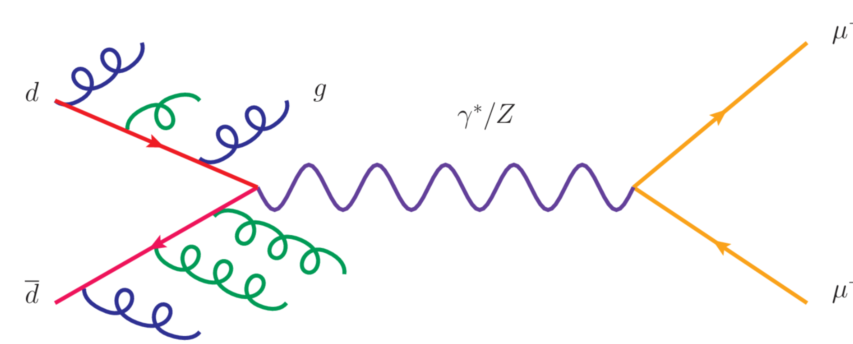

$\mathcal{O}(\alpha_{EW}^2\alpha_S^4)$ V+jets

PLB 834 (2022) 137438

Key ingredients

EVENT RECONSTRUCTION

Exploit the possibile topologies of the high jet-multiplicity events

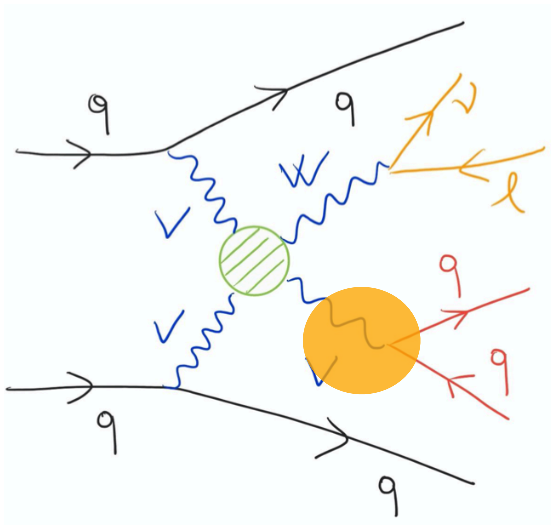

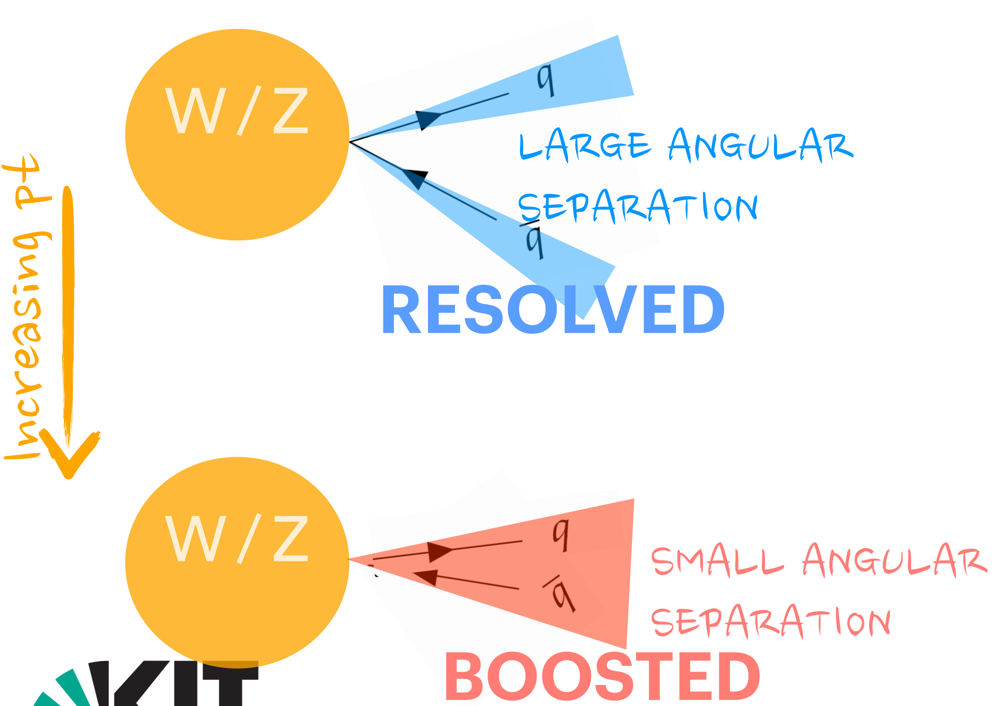

PLB 834 (2022) 137438

Key ingredients

EVENT RECONSTRUCTION

Exploit the possibile topologies of the high jet-multiplicity events

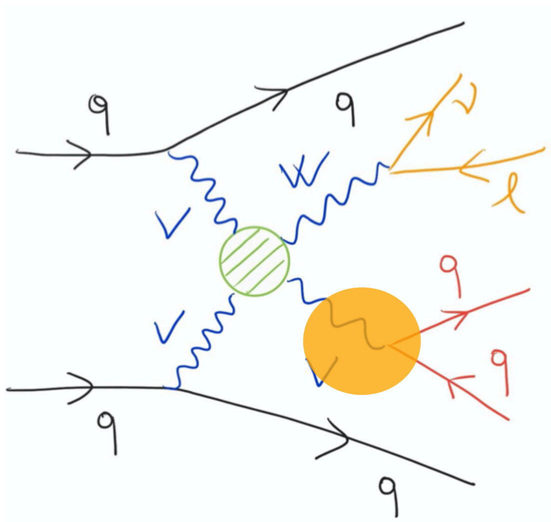

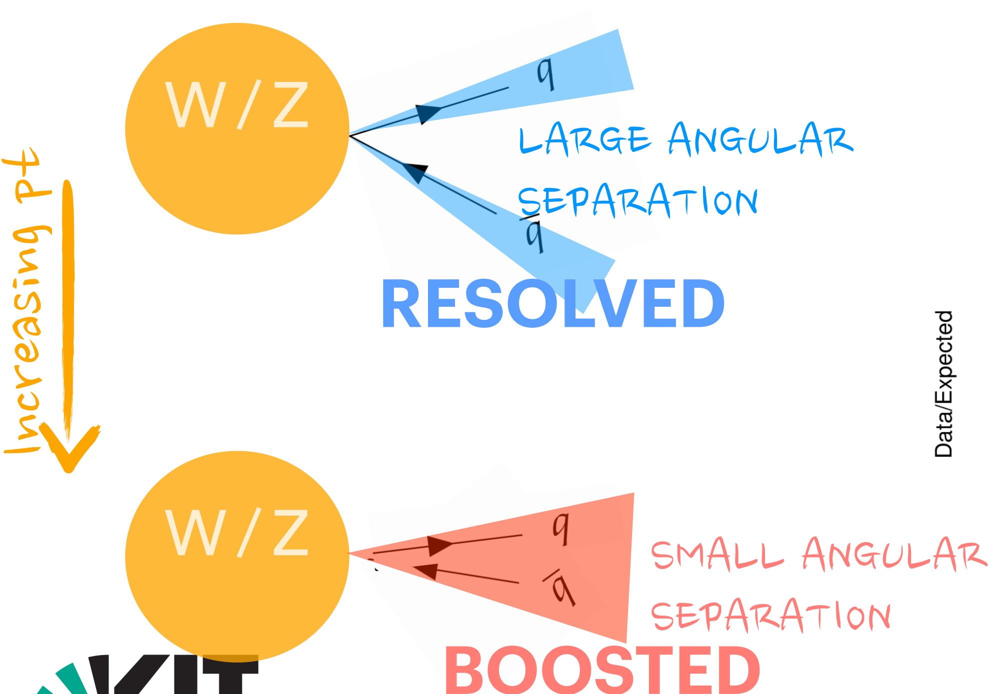

BKG MODELING

Definition of a series of free floating parameters per topology in the ML fit, to perfect the **modeling of VBS-jets kinematics for W+jets background**

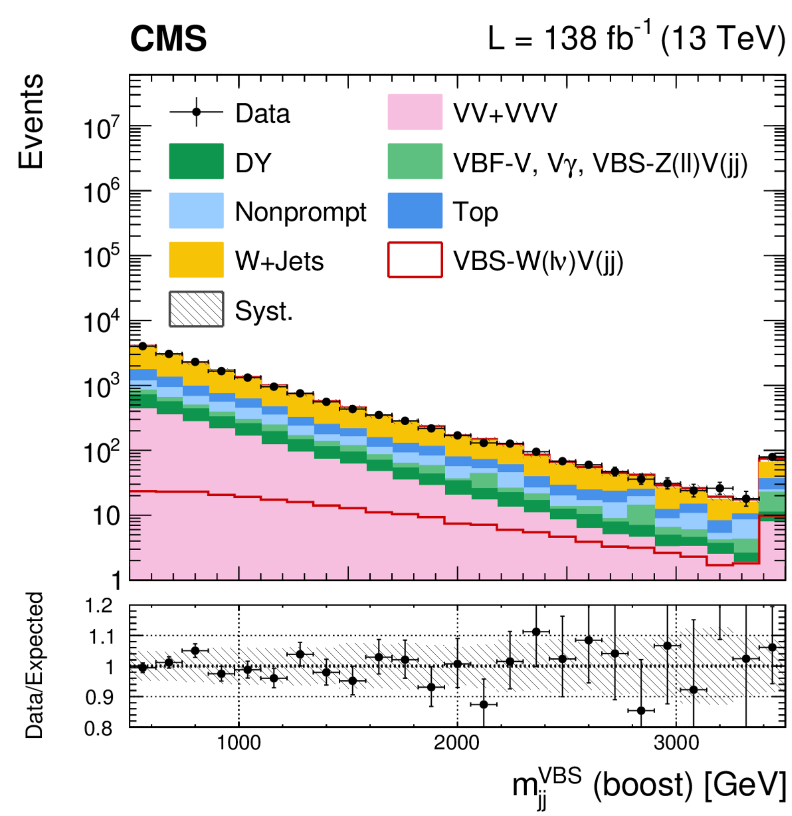

PLB 834 (2022) 137438

Key ingredients

EVENT RECONSTRUCTION

Exploit the possibile topologies of the high jet-multiplicity events

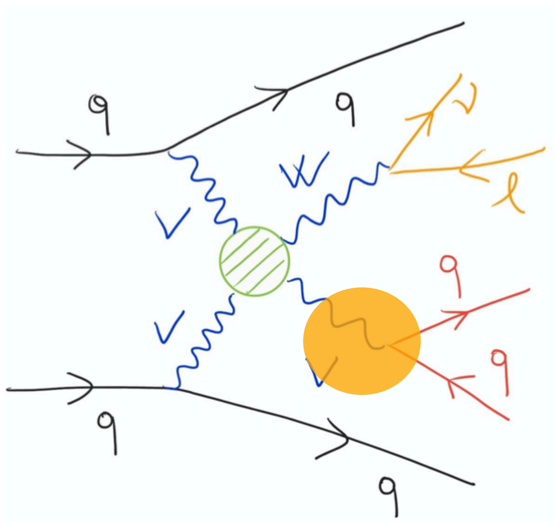

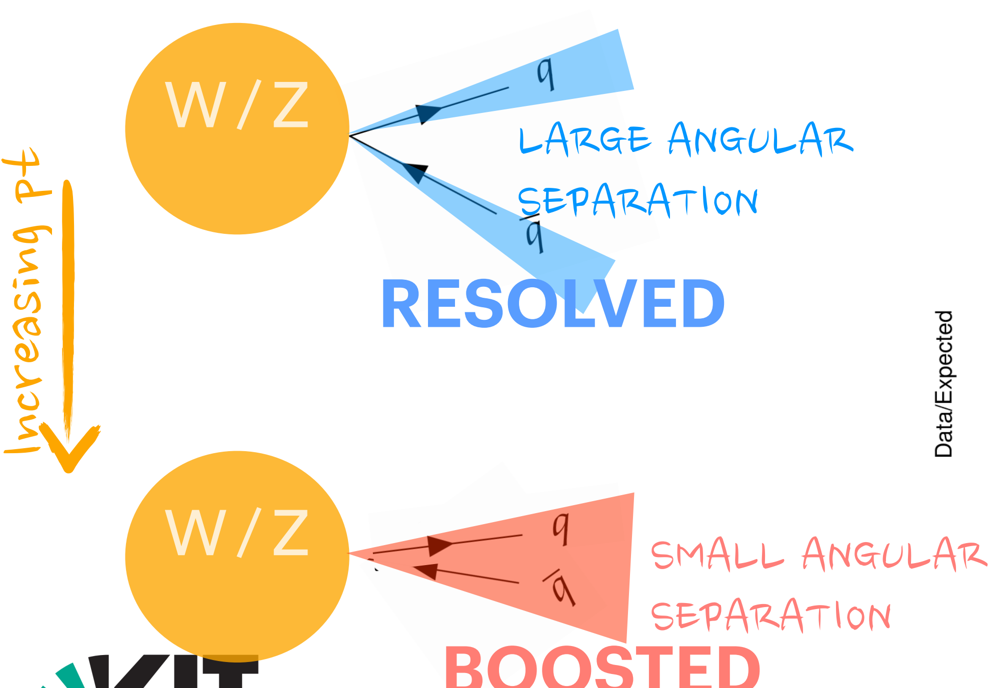

BKG MODELING

Definition of a series of free floating parameters per topology in the ML fit, to perfect the **modeling of VBS-jets kinematics for W+jets background**

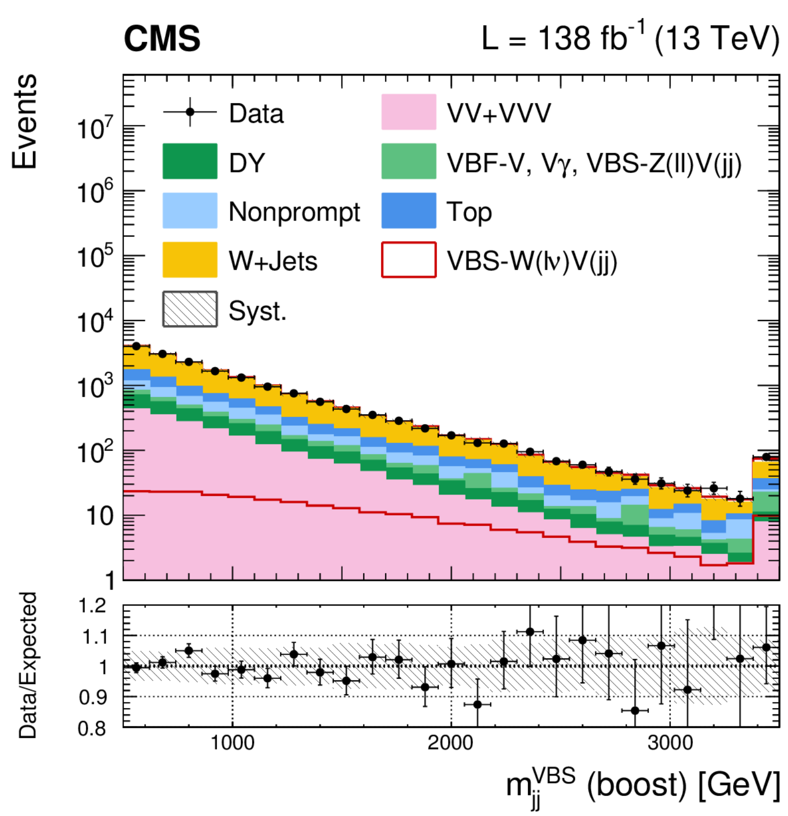

SIGNAL SEPARATION

DNN to optimize the sensitivity to the EW VBS process and separate the VBS signal from the large backgrounds

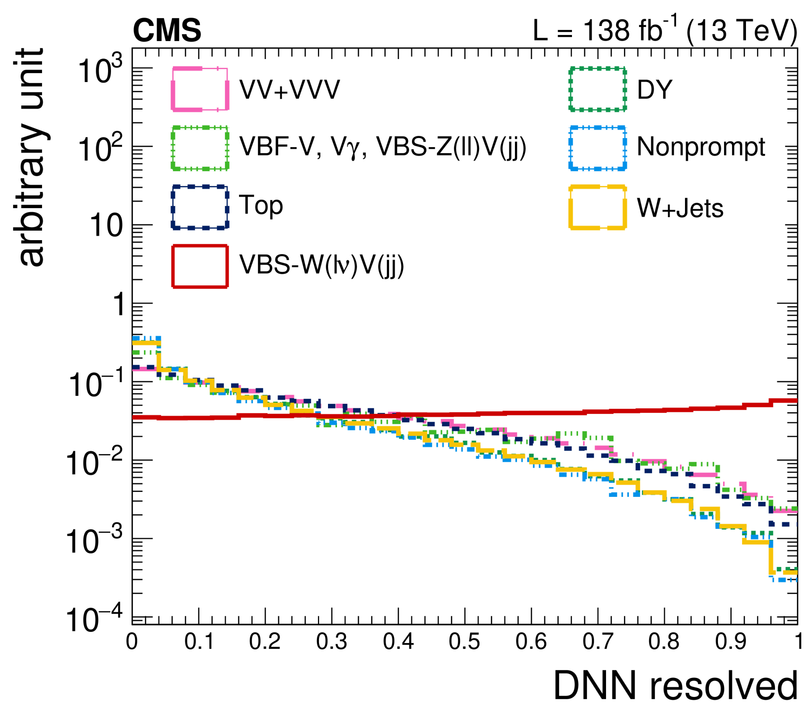

PLB 834 (2022) 137438

First evidence of semi-leptonic VBS

Three different measurements from the same data

PLB 834 (2022) 137438

First evidence of semi-leptonic VBS

Three different measurements from the same data

1. **SM electroweak signal strength:**

   - $\mu_{EW} = \sigma^{obs}/\sigma^{SM} = 0.85^{+0.24}_{-0.20} = {}^{+0.21}_{-0.17}(\text{ syst })^{+0.12}_{-0.12}(\text{ stat })$
   - **4.4 σ observed** (**5.1 expected**)
     observed fiducial cross-section 1.9±0.5 pb

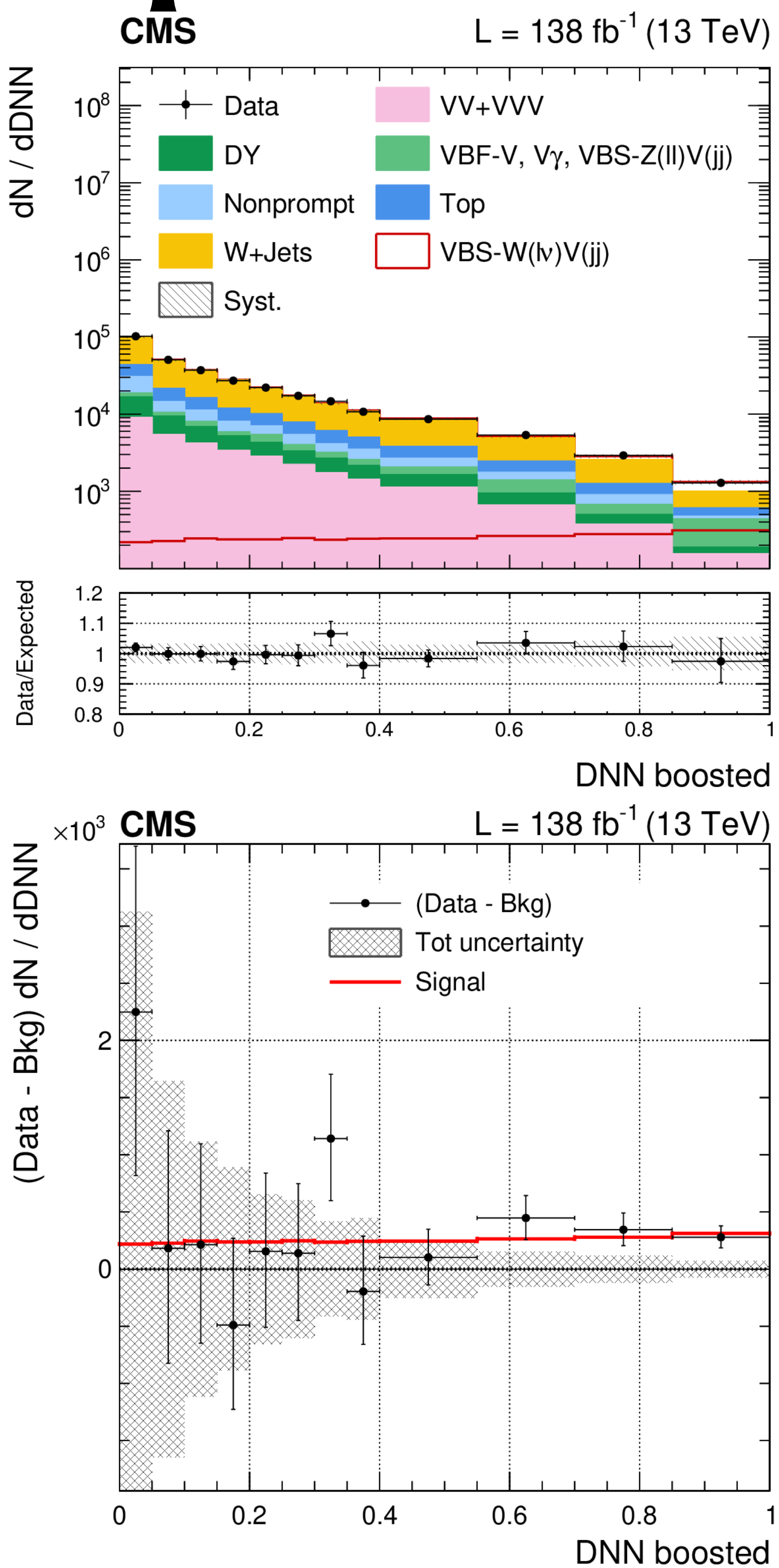

PLB 834 (2022) 137438

First evidence of semi-leptonic VBS

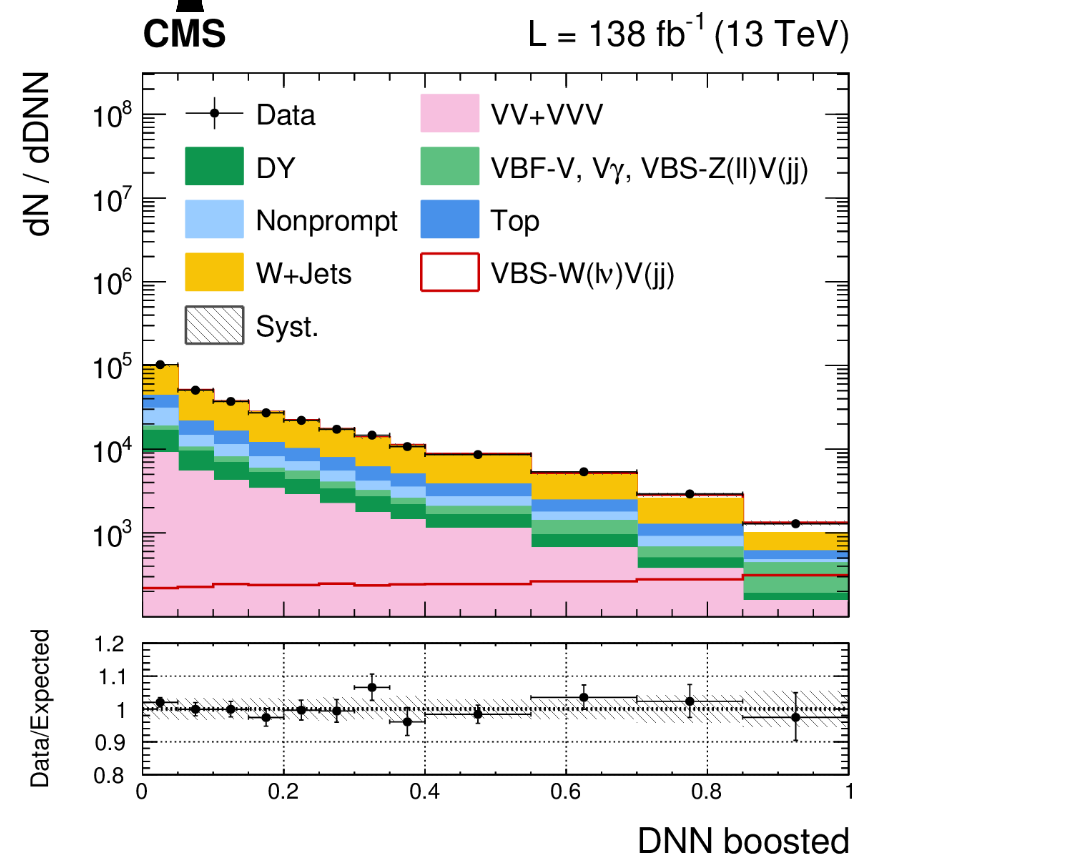

Three different measurements from the same data

1. **SM electroweak signal strength:**
   - $\mu_{EW} = \sigma^{obs}/\sigma^{SM} = 0.85^{+0.24}_{-0.20} = {}^{+0.21}_{-0.17}(\text{ syst })^{+0.12}_{-0.12}(\text{ stat })$
   - **4.4 σ observed** (**5.1 expected**)
     observed fiducial cross-section 1.9±0.5 pb
2. **Inclusive EW + QCD WV signal strength**:
   - $\mu_{EW+QCD} = \sigma^{obs}/\sigma^{SM} = 0.98^{+0.20}_{-0.17} = {}^{+0.19}_{-0.16}(\text{ syst })^{+0.07}_{-0.07}(\text{ stat })$
   - Total EW+QCD cross-section: $16.6\ ^{+3.4}_{-2.9}$ pb

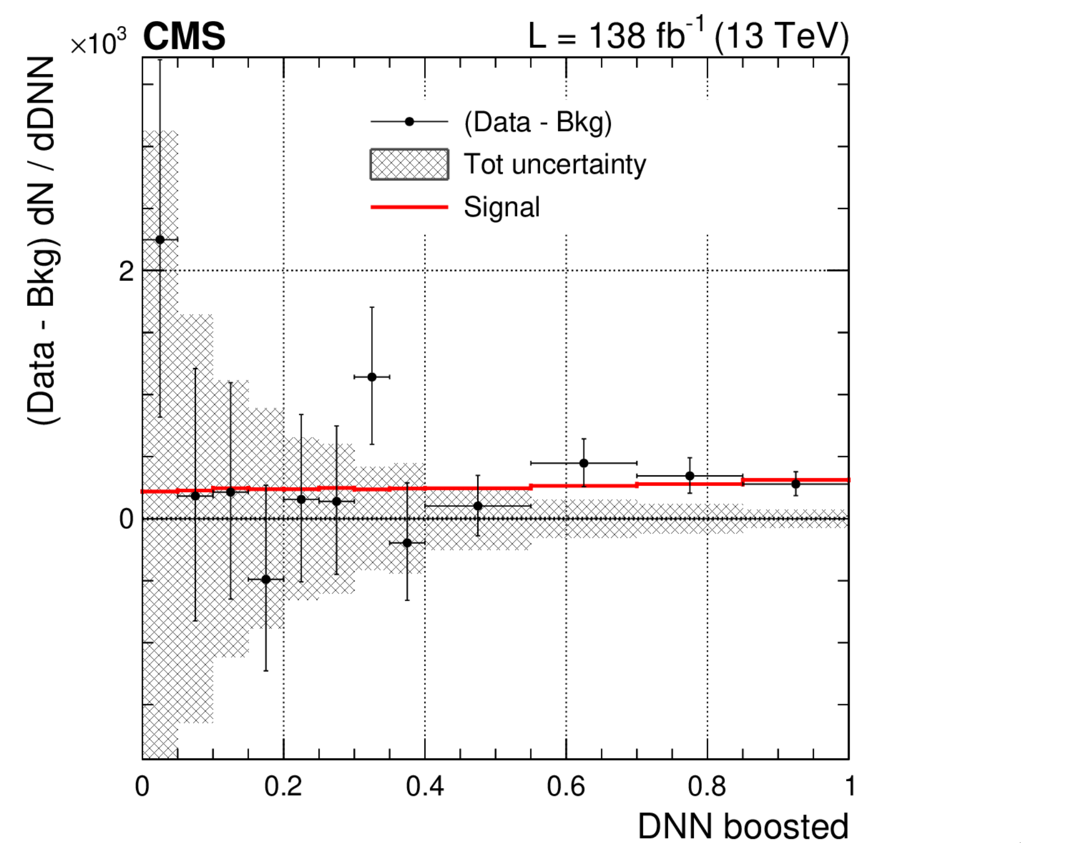

First evidence of semi-leptonic VBS

Three different measurements from the same data

1. **SM electroweak signal strength:**

   - $\mu_{EW} = \sigma^{obs}/\sigma^{SM} = 0.85^{+0.24}_{-0.20} = {}^{+0.21}_{-0.17}(\text{ syst })^{+0.12}_{-0.12}(\text{ stat}$
   - **4.4 σ observed** (**5.1 expected**)
     observed fiducial cross-section 1.9±0.5 pb

2. **Inclusive EW + QCD WV signal strength**:

   - $\mu_{EW+QCD} = \sigma^{obs}/\sigma^{SM} = 0.98^{+0.20}_{-0.17} = {}^{+0.19}_{-0.16}(\text{ syst })^{+0.07}_{-0.07}(\text{ stat}$
   - Total EW+QCD cross-section: $16.6\ ^{+3.4}_{-2.9}$ pb

3. **Simultaneous 2D fit of the EW and QCD WV measurement**

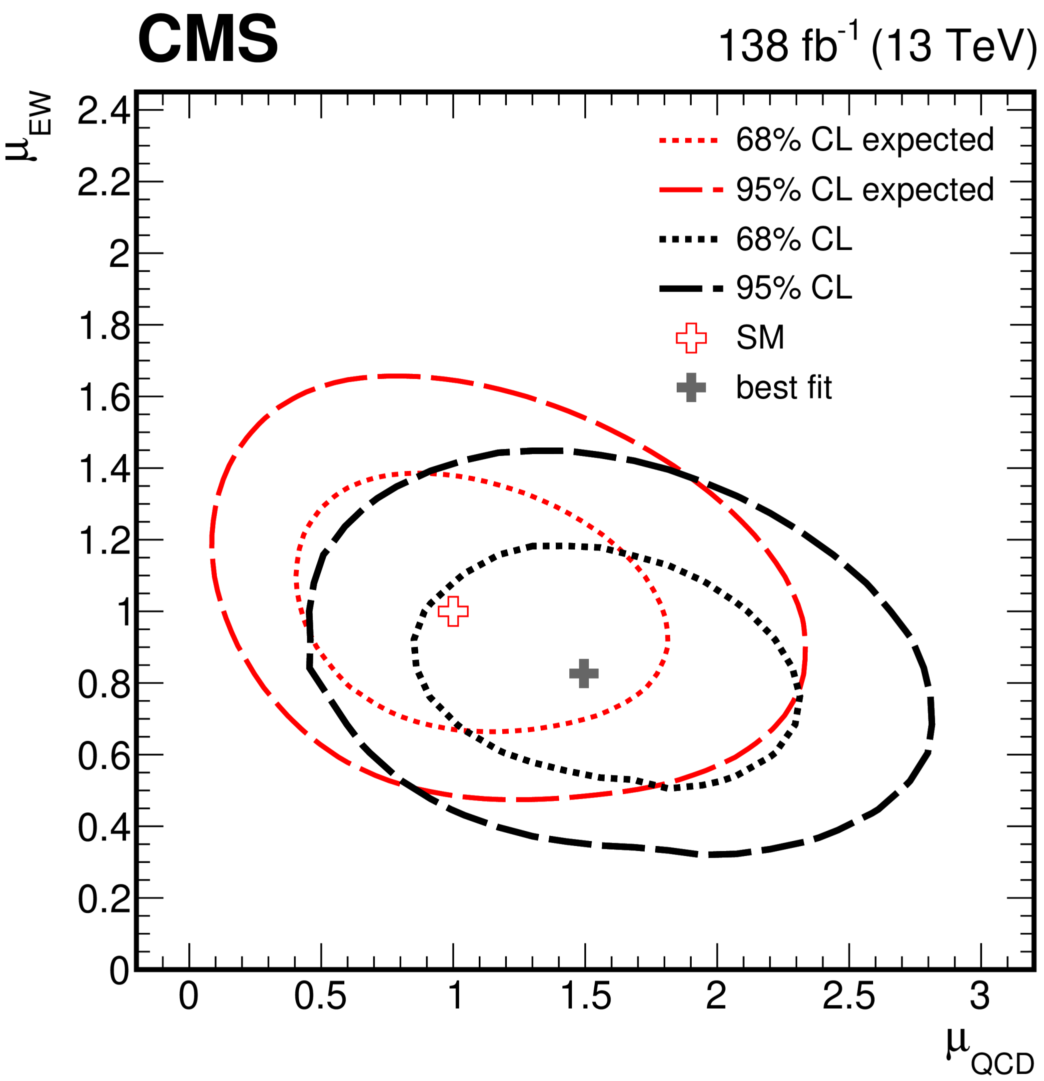

SUMMARY

- Highlights from CMS & ATLAS measurements in VBS
- Huge theoretical & experimental progress behind all these measurements
- Consistency tests of the SM and powerful tool to infer **new physics in a "UV-agnostic" way**
  - EFT dim-8, but global EFT fit as ultimate goal for future analyses
- **Many new analyses under implementation**
- Run3/4 are ahead, but many **interesting results from Run 2 are yet to come!**

ATLAS-CONF-2023-024

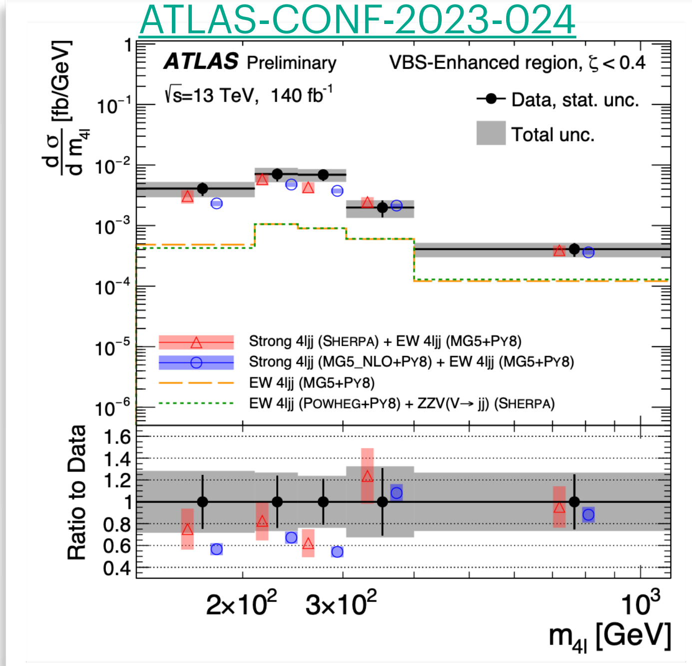

[link to recent ATLAS results]

arXiv:2211.16320

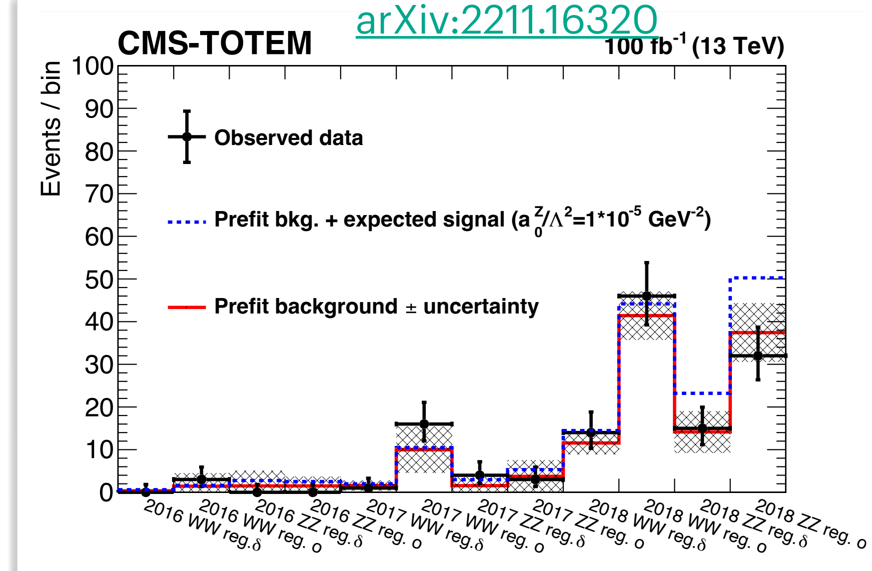

[link to recent CMS results]

Backup.

CMS-PAS-SMP-22-008

VBS decaying to tau lepton

Table 1: Definition of the SR and four CRs. All regions are disjoint. The SR and three CRs (Nonprompt, $t\bar{t}$, OS) are selected from an inclusive lepton trigger; the QCD enriched CR (last row) is selected from a jet-based trigger.

Region	1 ℓ, 1 τ_h, no additional "loose" ℓ		
	same-sign (ℓ, τ_h)	$p_T^{miss} > 50\,GeV$	additional requirements
SR	✓	×	$M_{jj} > 500\,GeV$ b-tagged jet veto
Nonprompt CR	✓	×	
$t\bar{t}$ CR	×	✓	b-tagged jet ("medium")
OS CR	×	✓	b-tagged jet veto ("loose")
QCD-enriched CR	1 "loose" e, μ, or τ_h, no add. leptons, $p_T^{miss} \leq 50\,GeV$, $M_T(\ell, p_T^{miss}) < 50\,GeV$		

$$M_T(\ell, p_T^{miss}) \simeq \sqrt{2 p_T^{\ell} p_T^{miss} [1 - \cos\Delta\phi]},$$

$$M_{1T}^2 = \left(\sqrt{M_{\tau l}^2 + p_T^{\tau l\,2}} + p_T^{miss}\right)^2 - \left|\vec{p}_T^{\,\tau l} + \vec{p}_T^{\,miss}\right|^2, \quad (2)$$

$$M_{o1}^2 = \left(p_T^{\tau} + p_T^{l} + p_T^{miss}\right)^2 - \left|\vec{p}_T^{\,\tau} + \vec{p}_T^{\,l} + \vec{p}_T^{\,miss}\right|^2. \quad (3)$$

The variable M_{1T} is the transverse mass of the $\tau\ell$ system with p_T^{miss}. For the second quantity, the τ and ℓ momenta and p_T^{miss} are projected in such a way the $\tau\ell$ system has a null invariant mass, and then the transverse mass of the three objects is obtained. The DNN implemented

Uncertainty source	$+\Delta\mu$	$-\Delta\mu$
Theory (PDF, QCD-scale, ISR, and FSR)	+0.157	−0.099
Non-prompt estimation	+0.136	−0.125
$t\bar{t}$ normalization	+0.051	−0.023
Prefiring	+0.105	−0.059
Luminosity	+0.079	−0.092
b-tagging and mistagging	+0.007	−0.004
Jet energy scale and resolution, Pile-up jet ID	+0.079	−0.097
Pileup	+0.152	−0.162
LO-to-NLO VBS corrections	+0.043	−0.025
Unclustered energy	+0.003	−0.010
Hadronic tau energy scale and DeepTau	+0.154	−0.152
Charge misidentification	+0.005	−0.010
Lepton reconstruction, identification, and isolation	+0.005	−0.024
MC statistical	+0.324	−0.322
Total systematic uncertainty	+0.344	−0.302
Data statistical uncertainty	+0.522	−0.477
Total uncertainty	+0.625	−0.564

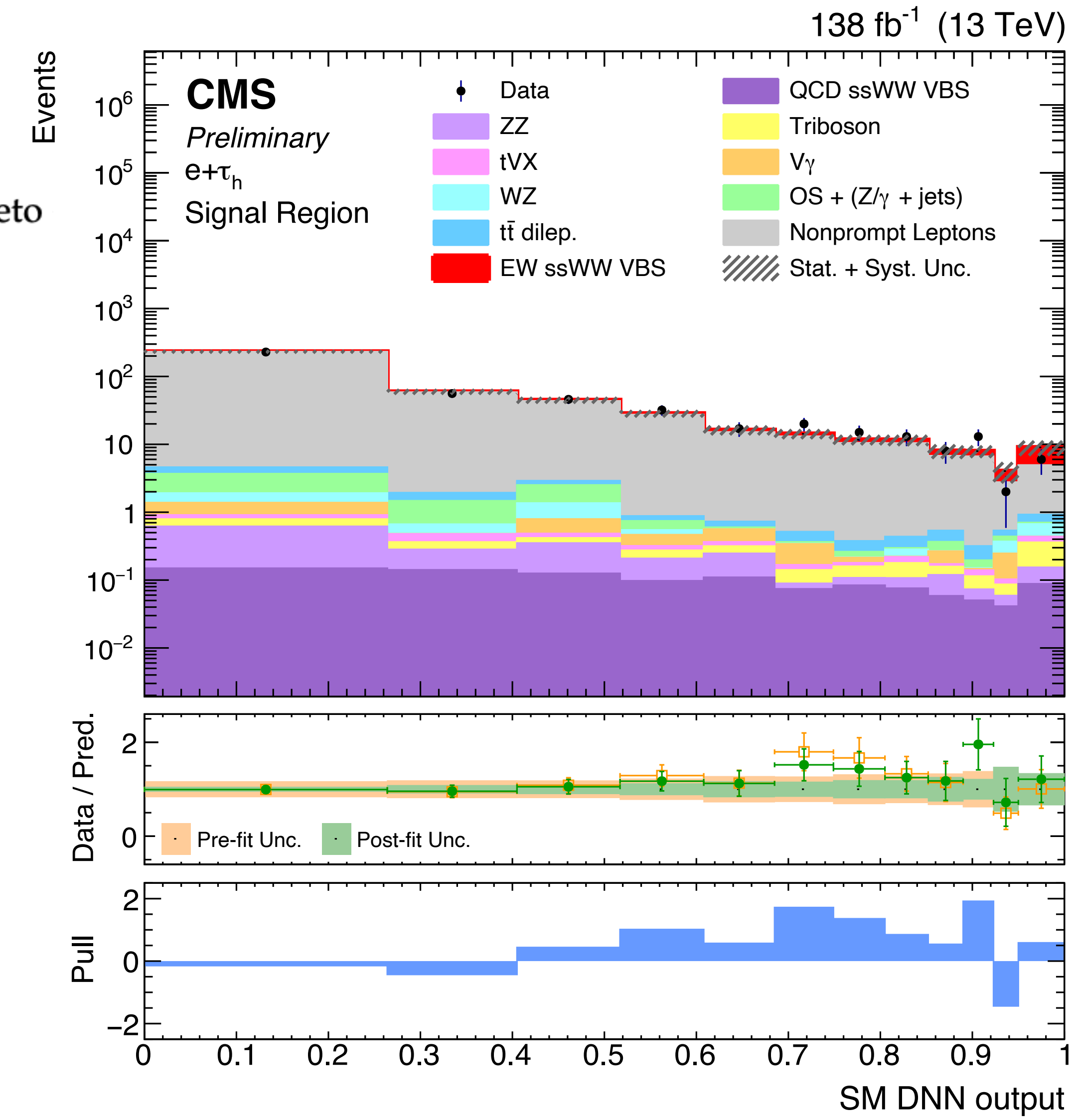

Opposite sign WW

Final state SR: **Opposite flavor**, positive centrality, 2-3 jets with veto on jets from b-quark

Sources	$\frac{\sqrt{(\Delta\mu)^2-(\Delta\mu')^2}}{\mu}$ (%)
Monte Carlo statistical uncertainty	7.7
Top quark theoretical uncertainties	6.3
Signal theoretical uncertainties	5.8
Jet experimental uncertainties	4.9
Strong W^+W^-jj theoretical uncertainties	1.3
Luminosity	0.8
Mis-identified lepton uncertainty	0.5
b-tagging	0.4
Lepton experimental uncertainties	0.1
Others	0.3
Data statistical uncertainty	12.3
Top quark normalisation uncertainty	4.9
Strong W^+W^-jj normalisation uncertainty	2.2
Total uncertainty	18.5

Category	Requirements
Leptons	$p_T > 27$ GeV $\|\eta\| < 2.47$ excluding $1.37 < \|\eta\| < 1.52$ (electrons) $\|\eta\| < 2.5$ (muons) Identification: `TightLH` (electrons), `Tight` (muons) Isolation: `Gradient` (electrons), `Tight_FixedRad` (muons) $\|d_0/\sigma_{d_0}\| < 5$ (electrons), $\|d_0/\sigma_{d_0}\| < 3$ (muons) $\|z_0 \sin\theta\| < 0.5$ mm
b-jets	$p_T > 20$ GeV and $\|\eta\| < 2.5$ (`DL1r` *b*-tagging with 85% efficiency)
Jets	$p_T > 25$ GeV and $\|\eta\| < 4.5$
Events	One electron and one muon with opposite electric charges No additional lepton with $p_T > 10$ GeV, `Loose` isolation, `TightLH/MediumLH` (electrons) and `Loose` (muons) identification $\zeta > 0.5$ $m_{e\mu} > 80$ GeV $E_T^{miss} > 15$ GeV Two or three jets No *b*-jet

Fully leptonic ssWW

Process, short description	ME Generator + parton shower	Order	Tune	PDF set in ME
EW, Int, QCD $W^{\pm}W^{\pm}jj$, nominal signal	MadGraph5_aMC@NLO2.6.7 + Herwig7.2	LO	default	NNPDF3.0nlo
EW, Int, QCD $W^{\pm}W^{\pm}jj$, alternative shower	MadGraph5_aMC@NLO2.6.7 + Pythia8.244	LO	A14	NNPDF3.0nlo
EW $W^{\pm}W^{\pm}jj$, NLO pQCD approx.	Sherpa2.2.11[2]	+0,1j@LO	Sherpa	NNPDF3.0nnlo
EW $W^{\pm}W^{\pm}jj$, NLO pQCD approx.	Powheg Boxv2 + Pythia8.230	NLO (VBS approx.)	AZNLO	NNPDF3.0nlo
QCD $W^{\pm}W^{\pm}jj$, NLO pQCD approx.	Sherpa2.2.2	+0,1j@LO	Sherpa	NNPDF3.0nnlo
QCD $VVjj$	Sherpa2.2.2	+0,1j@NLO; +2,3j@LO	Sherpa	NNPDF3.0nnlo
EW $W^{\pm}Zjj$	MadGraph5_aMC@NLO2.6.2+Pythia8.235	LO	A14	NNPDF3.0nlo
EW $ZZjj$	Sherpa2.2.2	LO	Sherpa	NNPDF3.0nnlo
QCD $V\gamma jj$	Sherpa2.2.11	+0,1j@NLO; +2,3j@LO	A14	NNPDF3.0nnlo
EW $V\gamma jj$	MadGraph5_aMC@NLO2.6.5+Pythia8.240	LO	A14	NNPDF3.0nlo
VVV	Sherpa2.2.1 (leptonic) & Sherpa2.2.2 (one $V \to jj$)	+0,1j@LO	Sherpa	NNPDF3.0nnlo
$t\bar{t}V$	MadGraph5_aMC@NLO2.3.3.p0 + Pythia8.210	NLO	A14	NNPDF3.0nlo

Fully leptonic ssWW

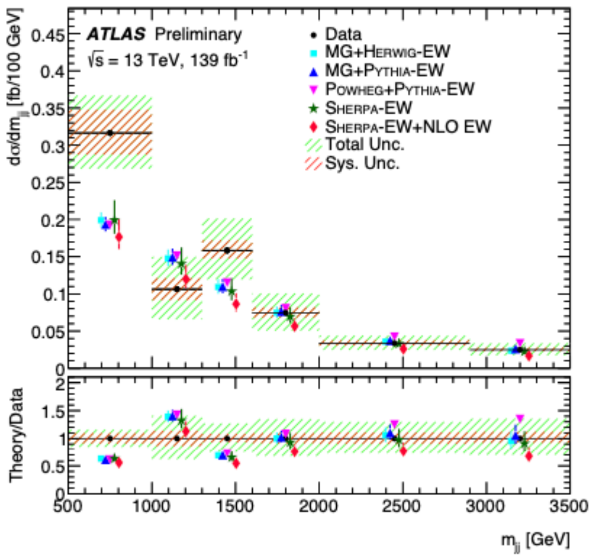

(c)

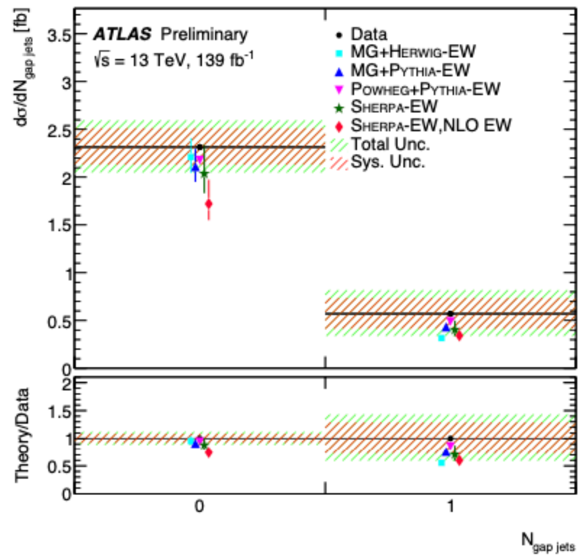

(d)

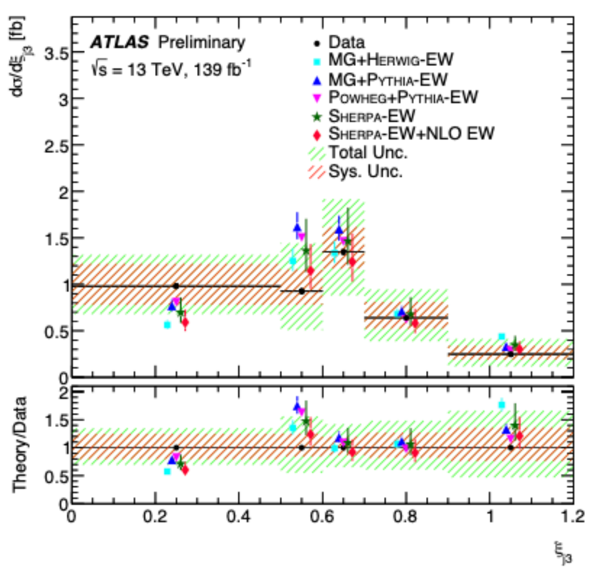

(e)

Source	Impact [%]
Experimental	
Electron calibration	0.4
Muon calibration	0.5
Jet energy scale and resolution	1.5
$E_{\mathrm{T}}^{\mathrm{miss}}$ scale and resolution	0.1
b-tagging inefficiency	0.7
Background, misid. leptons	3.1
Background, charge misrec.	0.6
Pileup modelling	0.1
Luminosity	1.8
Modelling	
$W^{\pm}W^{\pm}jj$ shower, scale, PDF & α_s	0.7
EW $W^{\pm}W^{\pm}jj$, QCD corrections	3.6
EW $W^{\pm}W^{\pm}jj$, EW corrections	0.4
QCD $W^{\pm}W^{\pm}jj$, QCD corrections	0.1
Background, WZ scale, PDF & α_s	0.4
Background, WZ reweighting	1.3
Background, other	1.0
Model statistical	1.6
Experimental and modelling	5.9
Data statistical	6.6
Total	8.9

Figure 5: Fiducial differential cross sections of EW $W^{\pm}W^{\pm}jj$ production as a function of (a) $m_{\ell\ell}$, (b) m_{T}, (c) m_{jj}, (d) $N_{\mathrm{gap\ jets}}$, and (e) ξ_{j_3}. The measured data are shown as black points with horizontal bars indicating the bin range and red (green) hatched boxes representing the statistical (total) uncertainty. The data are compared to a number of Standard Model predictions as described in the text. For the predictions where vertical error bars are shown, they correspond to the uncertainty coming from the variations of the renormalisation and factorisation scales, PDF and α_s. Overflow events are included in the last bin. The lower panel of each plot shows the ratio between the predicted and measured cross sections.

ssWW and BSM

DIRECT PROBE

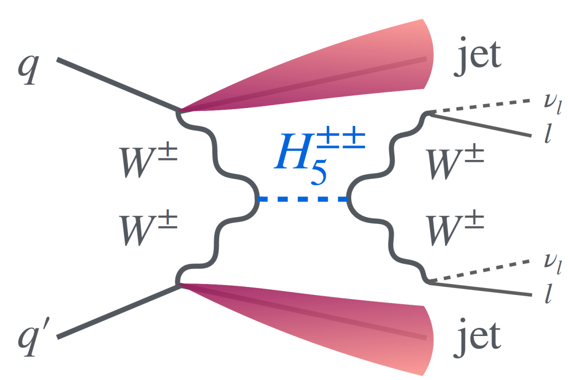

Possible new doubly-charged boson in the **s-channel**, tested with **transverse mass**.

Local excess of events over the SM prediction consistent with a $H^{\pm\pm}$ boson of mass of about 450 GeV

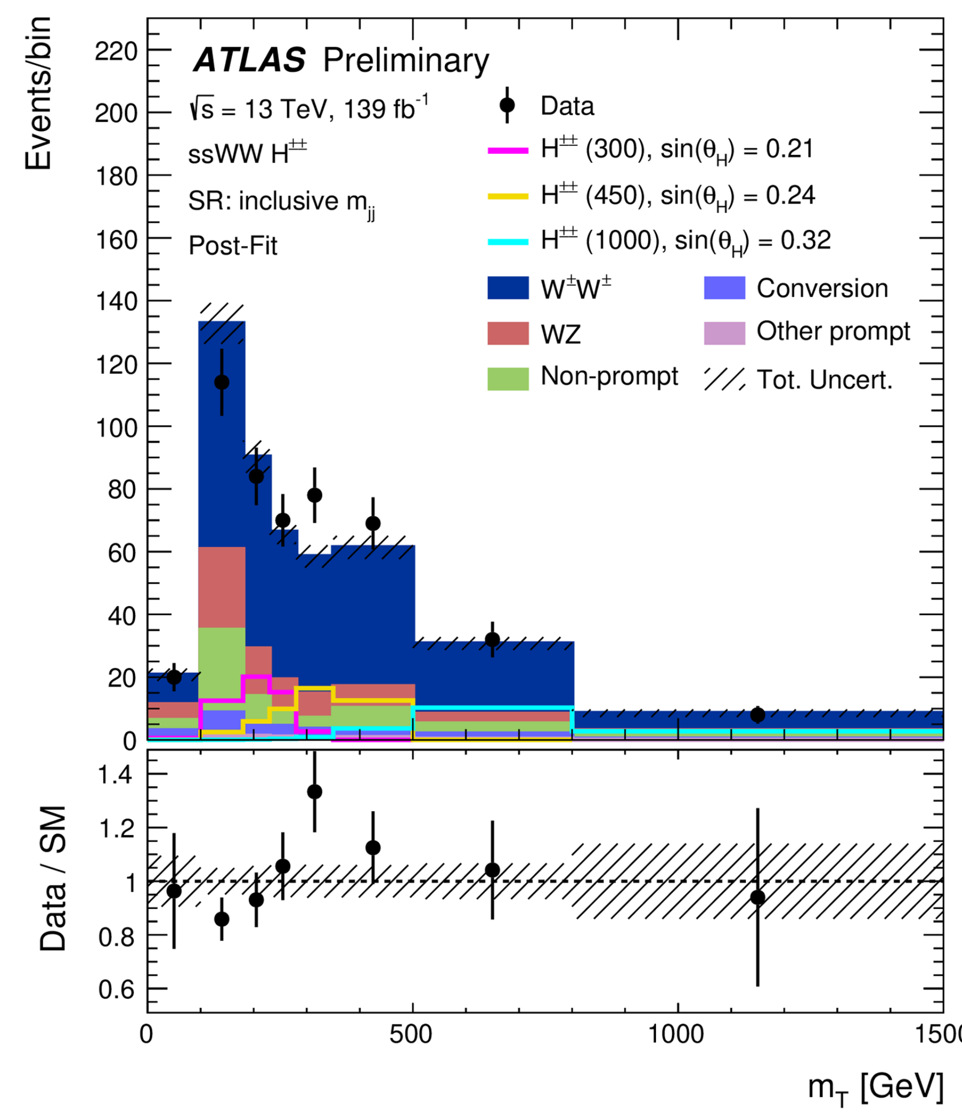

Global significance of 2.5σ

Stringent constraints on the Georgi-Machacek model

ssWW and BSM

INDIRECT PROBE

Table 7: Expected and observed limits on the Wilson coefficients for various operators without any unitarisation procedure and with a unitarisation cut-off at the unitarity bound. The unitarity bounds for each operator as a function of the cut-off scale are defined for one non-zero Wilson coefficient following Ref. [72]. The last column represents lower and upper limits at the respective cut-off value, where the unitarity bound and experimental bound are crossing. Cases where no crossing with the unitarity bound was found in the scanned region above 600 GeV are labelled by "–". The notation S02 is used to indicate that the coefficients corresponding to the operators O_{S0} and O_{S2} are assigned the same value. The limits on M7 were obtained without taking into account the SM-EFT interference for the EW $W^{\pm}Zjj$ final state.

Coefficient	Type	No unitarisation cut-off [TeV^{-4}]	Lower and upper limit at the respective unitarity bound [TeV^{-4}]
f_{M0}/Λ^4	exp.	[-3.9, 3.8]	-64 at 0.9 TeV, 40 at 1.0 TeV
	obs.	[-4.1, 4.1]	-140 at 0.7 TeV, 117 at 0.8 TeV
f_{M1}/Λ^4	exp.	[-6.3, 6.6]	-25.5 at 1.6 TeV, 31 at 1.5 TeV
	obs.	[-6.8, 7.0]	-45 at 1.4 TeV, 54 at 1.3 TeV
f_{M7}/Λ^4	exp.	[-9.3, 8.8]	-33 at 1.8 TeV, 29.1 at 1.8 TeV
	obs.	[-9.8, 9.5]	-39 at 1.7 TeV, 42 at 1.7 TeV
f_{S02}/Λ^4	exp.	[-5.5, 5.7]	-94 at 0.8 TeV, 122 at 0.7 TeV
	obs.	[-5.9, 5.9]	–
f_{S1}/Λ^4	exp.	[-22.0, 22.5]	–
	obs.	[-23.5, 23.6]	–
f_{T0}/Λ^4	exp.	[-0.34, 0.34]	-3.2 at 1.2 TeV, 4.9 at 1.1 TeV
	obs.	[-0.36, 0.36]	-7.4 at 1.0 TeV, 12.4 at 0.9 TeV
f_{T1}/Λ^4	exp.	[-0.158, 0.174]	-0.32 at 2.6 TeV, 0.44 at 2.4 TeV
	obs.	[-0.174, 0.186]	-0.38 at 2.5 TeV, 0.49 at 2.4 TeV
f_{T2}/Λ^4	exp.	[-0.56, 0.70]	-2.60 at 1.7 TeV, 10.3 at 1.2 TeV
	obs.	[-0.63, 0.74]	–

HIGHER ORDER PREDICTIONS IN VBS

Table 1: Summary of higher-order predictions currently available for the ss-WW channel: at fixed order and matched to parton shower. The symbols ✓, ✓*, and X means that the corresponding predictions are available, in the VBS approximation, or not available yet.

Order	$\mathcal{O}(\alpha^7)$	$\mathcal{O}(\alpha_s\alpha^6)$	$\mathcal{O}({\alpha_s}^2\alpha^5)$	$\mathcal{O}({\alpha_s}^3\alpha^4)$
NLO	✓	✓	✓	✓
NLO+PS	✓	✓*	X	✓

Table 3: Summary of higher-order predictions currently available for the WZ channel: at fixed order and matched to parton shower. The symbols ✓, ✓*, and X means that the corresponding predictions are available, in the VBS approximation, or not yet.

Order	$\mathcal{O}(\alpha^7)$	$\mathcal{O}(\alpha_s\alpha^6)$	$\mathcal{O}({\alpha_s}^2\alpha^5)$	$\mathcal{O}({\alpha_s}^3\alpha^4)$
NLO	✓	✓	X	✓
NLO+PS	X	✓*	X	✓

Table 7: Summary of higher-order predictions currently available for the os-WW channel: at fixed order and matched to parton shower. The symbols ✓, ✓*, and X means that the corresponding predictions are available, in the VBS approximation, or not yet.

Order	$\mathcal{O}(\alpha^7)$	$\mathcal{O}(\alpha_s\alpha^6)$	$\mathcal{O}({\alpha_s}^2\alpha^5)$	$\mathcal{O}({\alpha_s}^3\alpha^4)$
NLO	X	✓*	X	✓
NLO+PS	X	✓*	X	✓

Table 5: Summary of higher-order predictions currently available for the ZZ channel: at fixed order and matched to parton shower. The symbols ✓, ✓*, and X means that the corresponding predictions are available, in the VBS approximation, or not yet.

Order	$\mathcal{O}(\alpha^7)$	$\mathcal{O}(\alpha_s\alpha^6)$	$\mathcal{O}({\alpha_s}^2\alpha^5)$	$\mathcal{O}({\alpha_s}^3\alpha^4)$
NLO	✓	✓	X	✓
NLO+PS	X	✓*	X	✓

Refs: arXiv:1708.00268 [hep-ph], arXiv:2102.10991 [hep-ph]

$W\gamma jj$ measurement

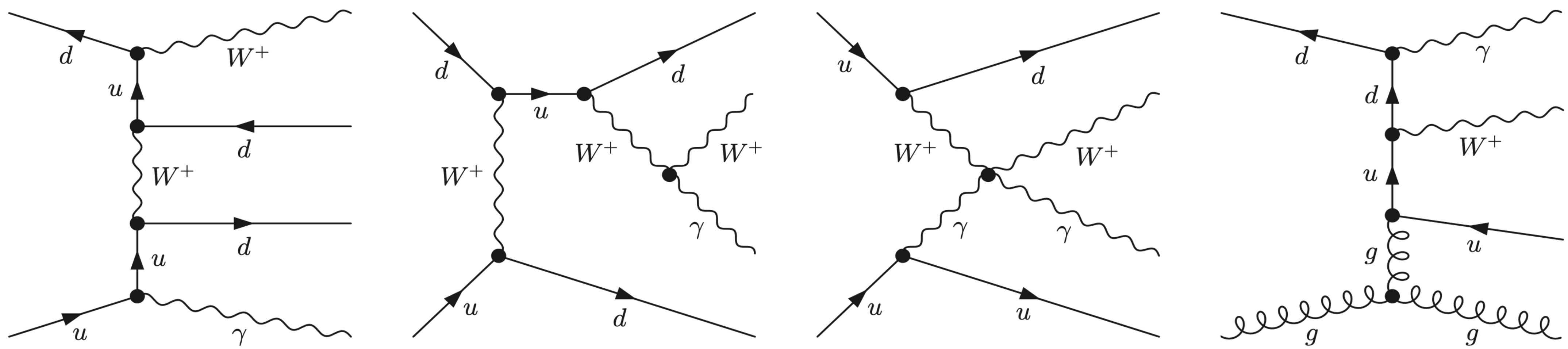

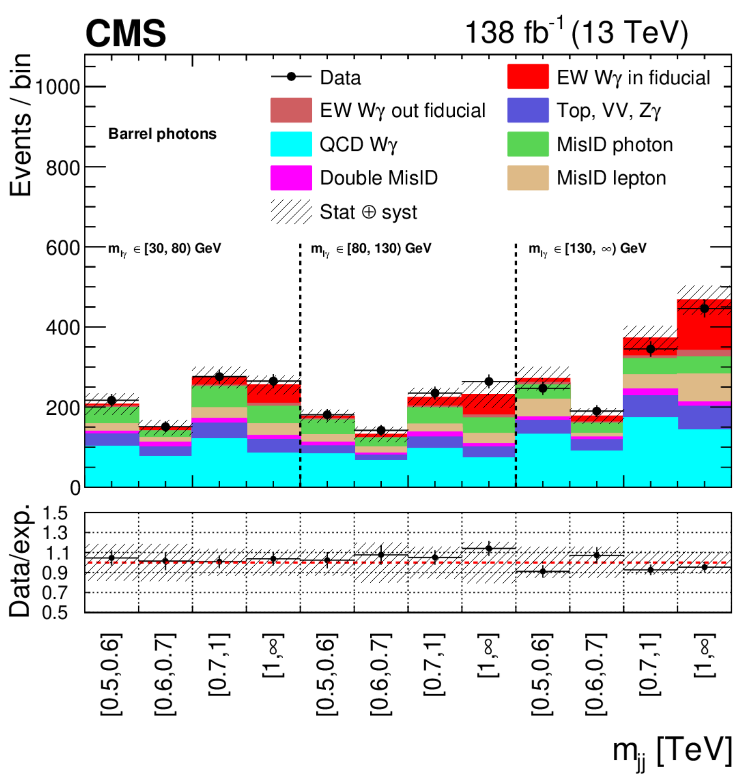

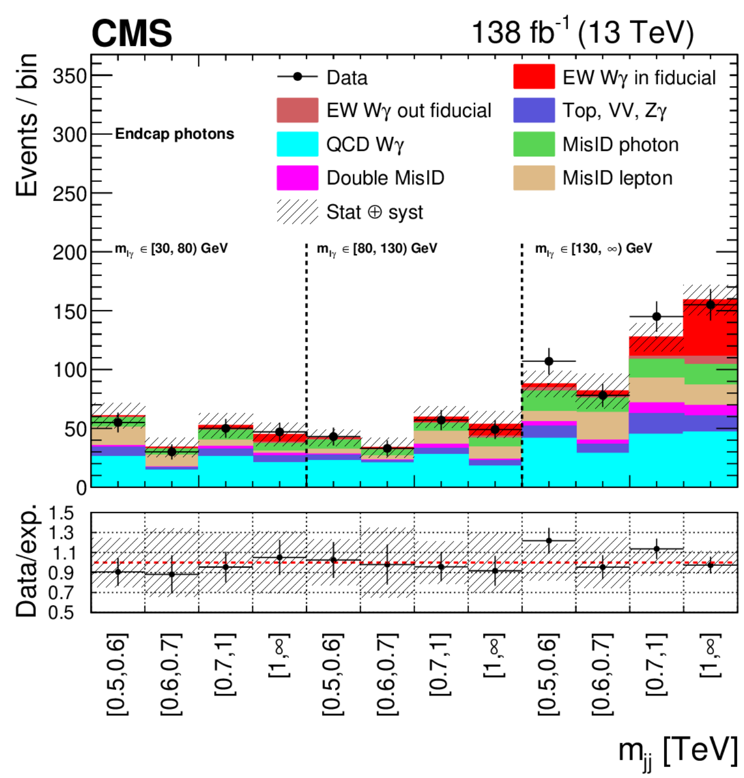

- The EWK $W\gamma jj$ production is observed with 6.03 σ (6.79 σ expected).
- Fiducial cross-section and differential cross-section are measured, using mjj,$ml\gamma$ 2D-fit

$$\sigma^{\text{fid}}_{\text{EW}} = 23.5 \pm 2.8\,(\text{stat})^{+1.9}_{-1.7}\,(\text{theo})^{+3.5}_{-3.4}\,(\text{syst})\text{ fb} = 23.5^{+4.9}_{-4.7}\text{ fb}.$$

$W\gamma jj$ measurement

- The EWK $W\gamma jj$ production can probe the EFT model via anomalous quartic gauge coupling (aQGC) effect. Strong constraints are set to EFT dim-8 parameters. Red rectangle contains the most stringent limits.

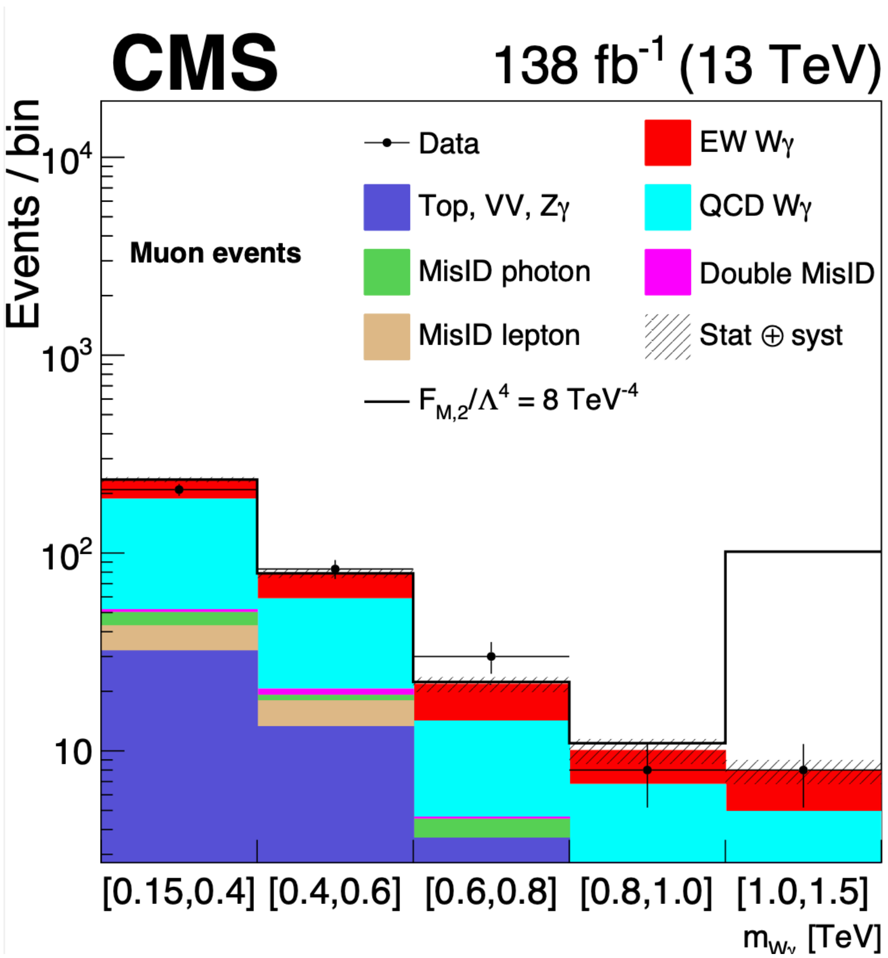

Expected limit	Observed limit	$\mathcal{U}_{\mathrm{bound}}$
$-5.1 < f_{M,0}/\Lambda^4 < 5.1$	$-5.6 < f_{M,0}/\Lambda^4 < 5.5$	1.7
$-7.1 < f_{M,1}/\Lambda^4 < 7.4$	$-7.8 < f_{M,1}/\Lambda^4 < 8.1$	2.1
$-1.8 < f_{M,2}/\Lambda^4 < 1.8$	$-1.9 < f_{M,2}/\Lambda^4 < 1.9$	2.0
$-2.5 < f_{M,3}/\Lambda^4 < 2.5$	$-2.7 < f_{M,3}/\Lambda^4 < 2.7$	2.7
$-3.3 < f_{M,4}/\Lambda^4 < 3.3$	$-3.7 < f_{M,4}/\Lambda^4 < 3.6$	2.3
$-3.4 < f_{M,5}/\Lambda^4 < 3.6$	$-3.9 < f_{M,5}/\Lambda^4 < 3.9$	2.7
$-13 < f_{M,7}/\Lambda^4 < 13$	$-14 < f_{M7}/\Lambda^4 < 14$	2.2
$-0.43 < f_{T,0}/\Lambda^4 < 0.51$	$-0.47 < f_{T,0}/\Lambda^4 < 0.51$	1.9
$-0.27 < f_{T,1}/\Lambda^4 < 0.31$	$-0.31 < f_{T,1}/\Lambda^4 < 0.34$	2.5
$-0.72 < f_{T,2}/\Lambda^4 < 0.92$	$-0.85 < f_{T,2}/\Lambda^4 < 1.0$	2.3
$-0.29 < f_{T,5}/\Lambda^4 < 0.31$	$-0.31 < f_{T,5}/\Lambda^4 < 0.33$	2.6
$-0.23 < f_{T,6}/\Lambda^4 < 0.25$	$-0.25 < f_{T,6}/\Lambda^4 < 0.27$	2.9
$-0.60 < f_{T,7}/\Lambda^4 < 0.68$	$-0.67 < f_{T,7}/\Lambda^4 < 0.73$	3.1